

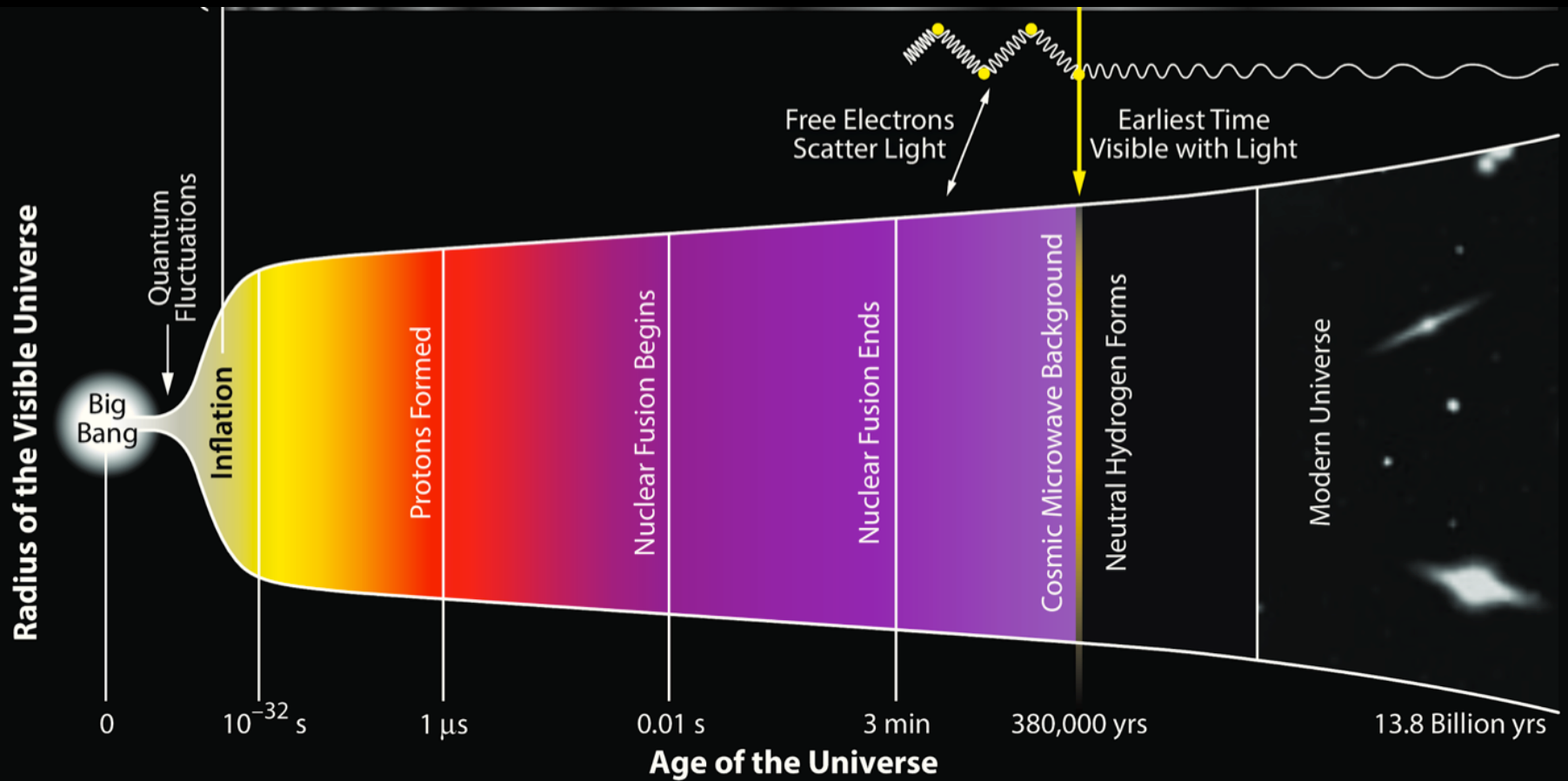
Detection of B-mode Polarization at Degree Scales using BICEP2

Angiola Orlando for the BICEP2 Collaboration



History of the Universe

Universe becomes transparent



The Sky at Millimeter Wavelengths

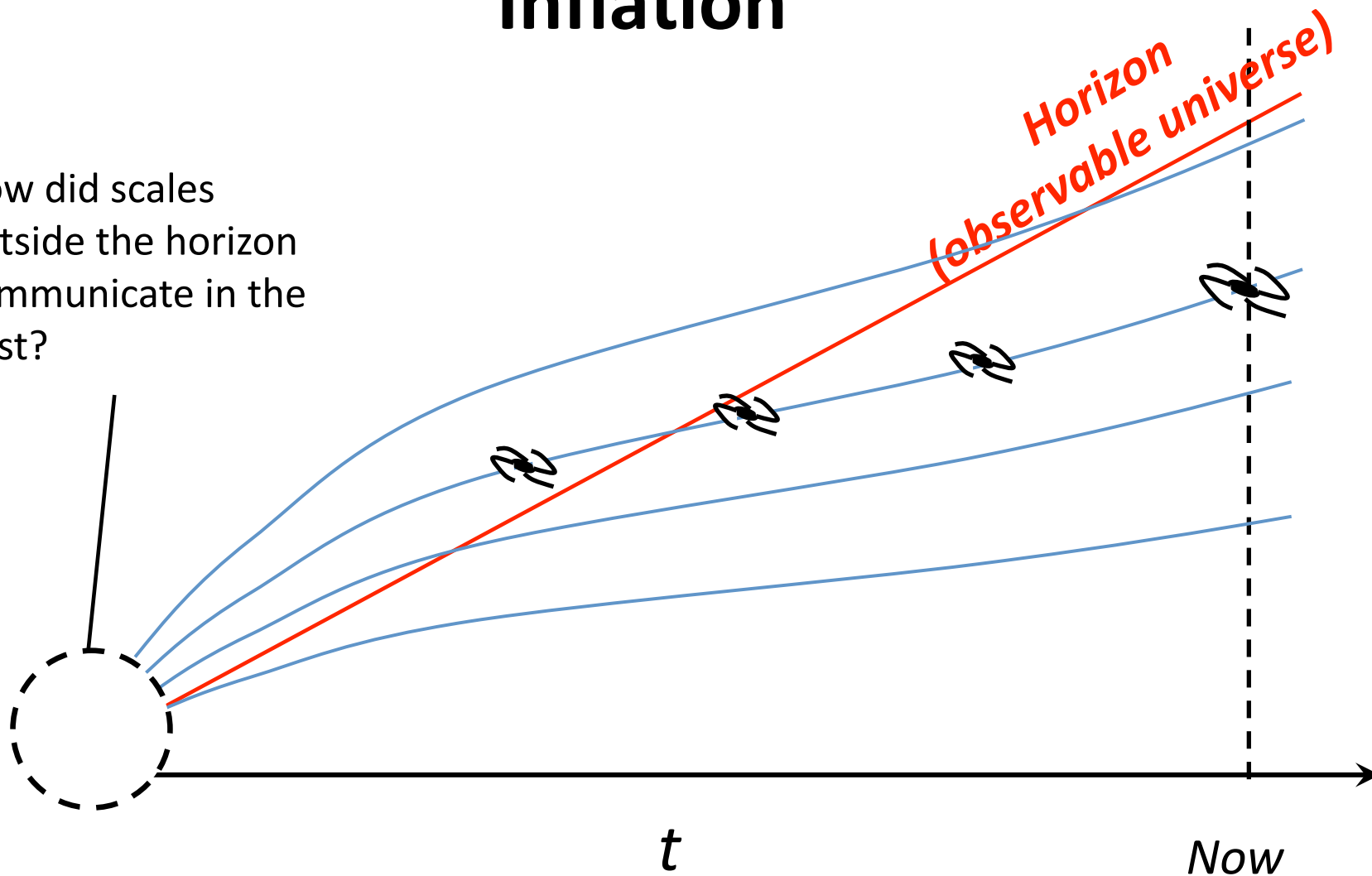


Every Direction is the SAME Temperature to ~10 ppm!

How Can This BE? A Deeply Troubling Question for Cosmologists in 1980...

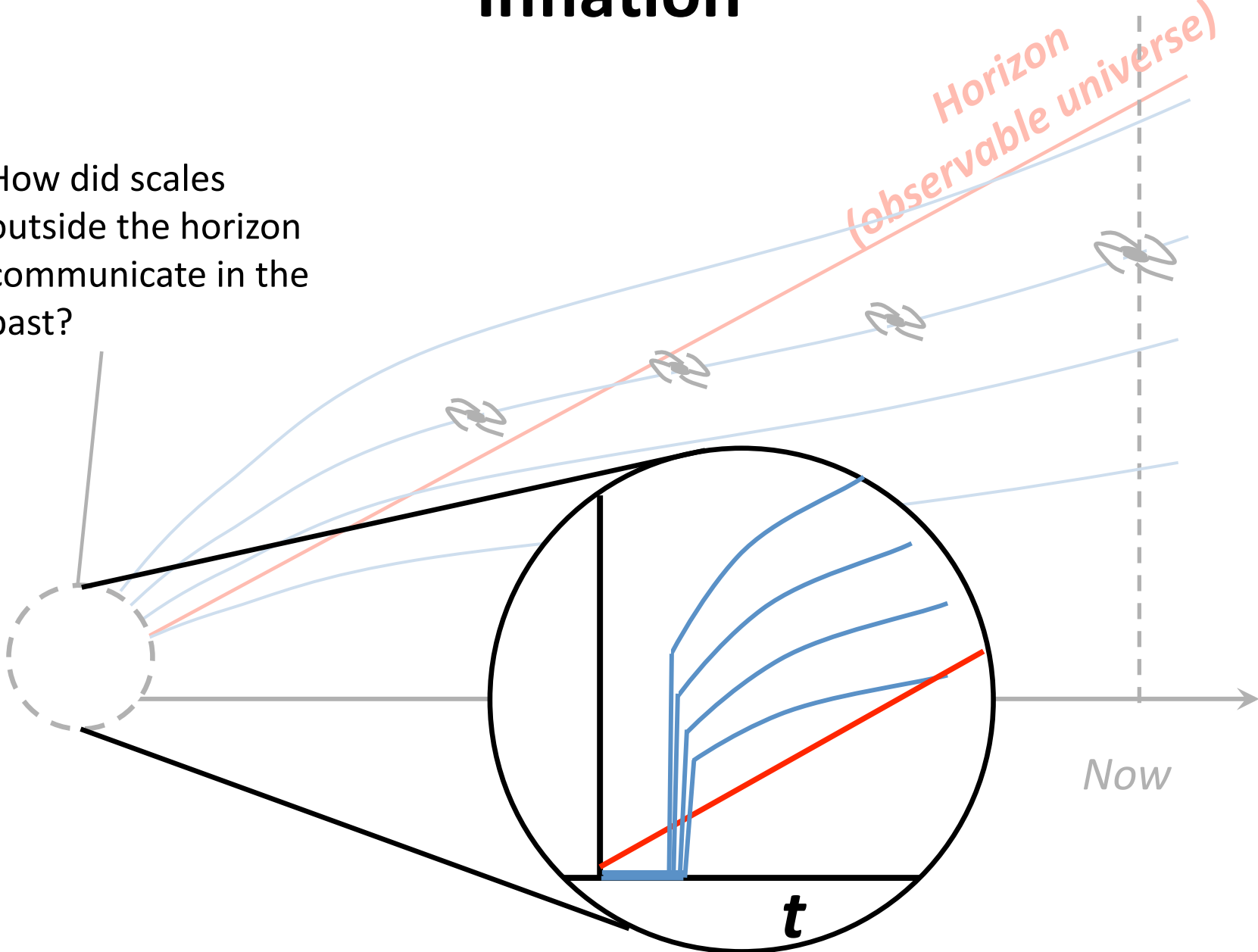
Inflation

How did scales
outside the horizon
communicate in the
past?



Inflation

How did scales outside the horizon communicate in the past?

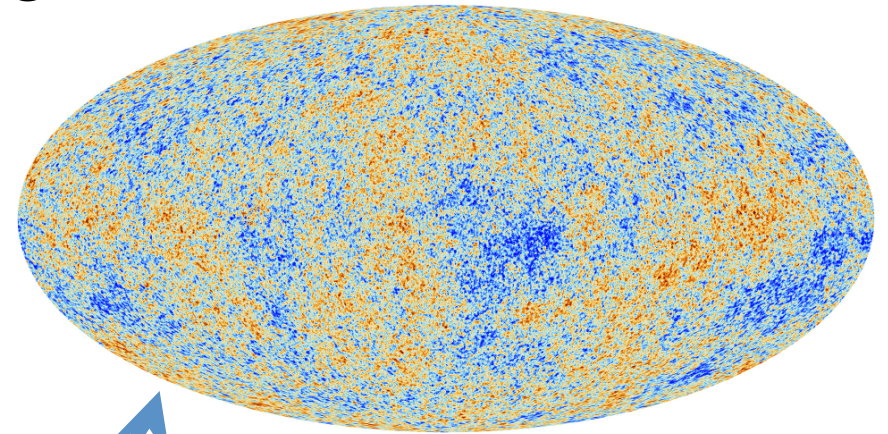


Density perturbations and gravitational waves

Sub-atomic vacuum fluctuations of "inflaton"

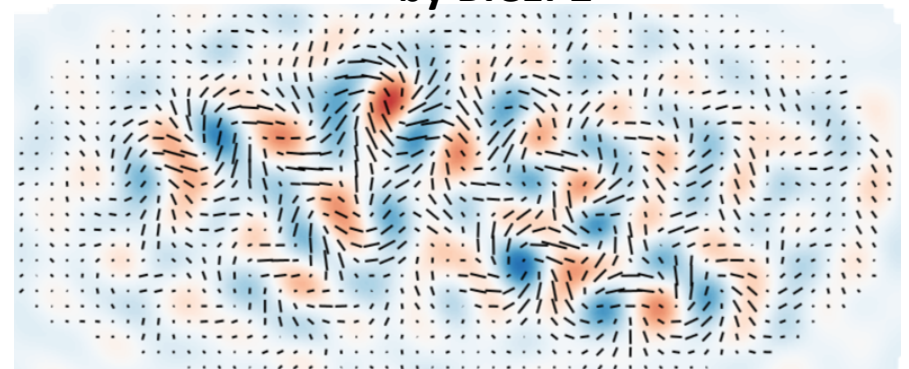


Sub-atomic vacuum fluctuations of *graviton* (quanta of gravity)



Density perturbations *studied* by Planck, WMAP, SPT, etc.

Gravitational waves detected by BICEP2

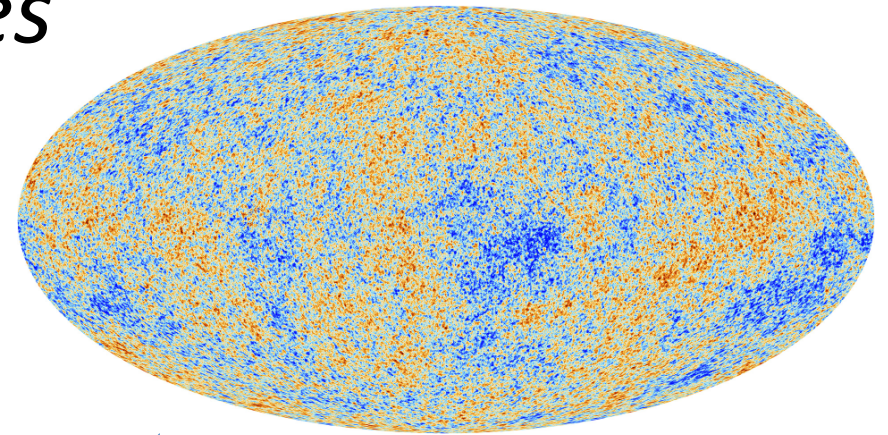


Density perturbations and gravitational waves

Sub-atomic vacuum fluctuations of "inflaton"



Sub-atomic vacuum fluctuations of *graviton* (quanta of gravity)

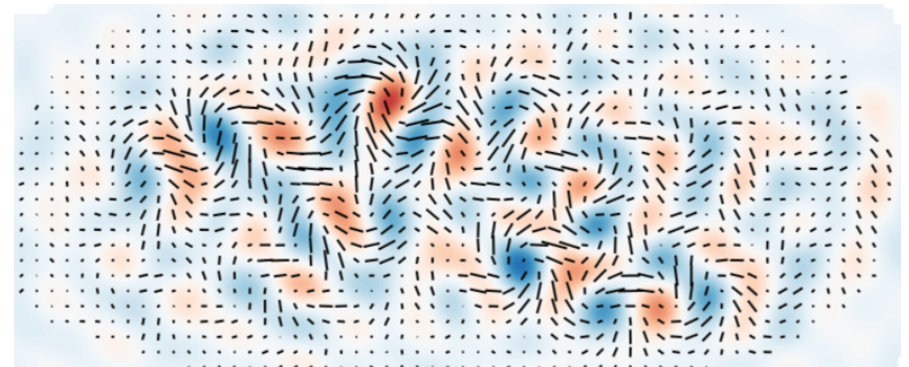


Density perturbations

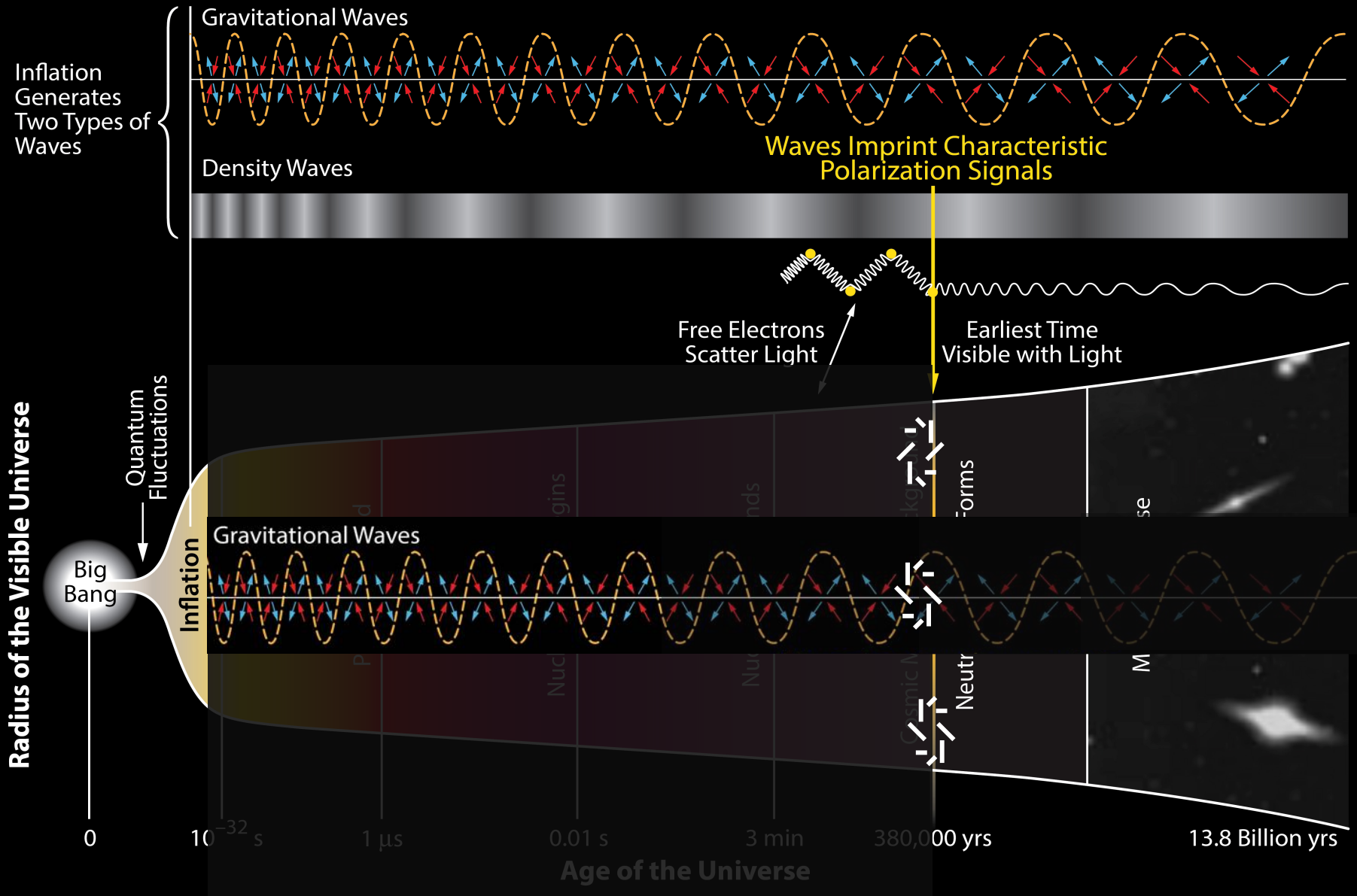
$$r \approx \frac{V[\phi]}{(4 \times 10^{16} \text{ GeV})^4}$$

GUT scale physics!?

Gravitational waves



History of the Universe

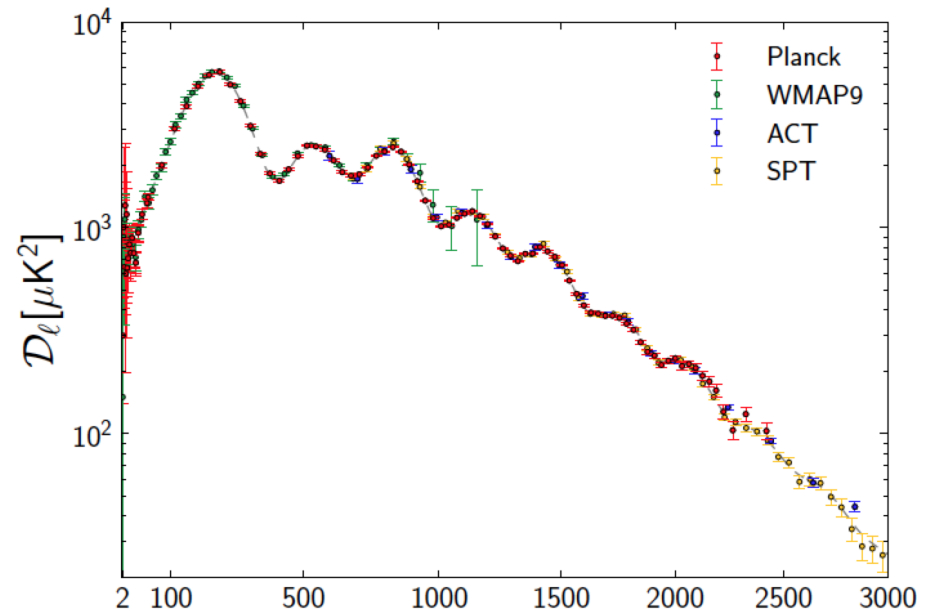
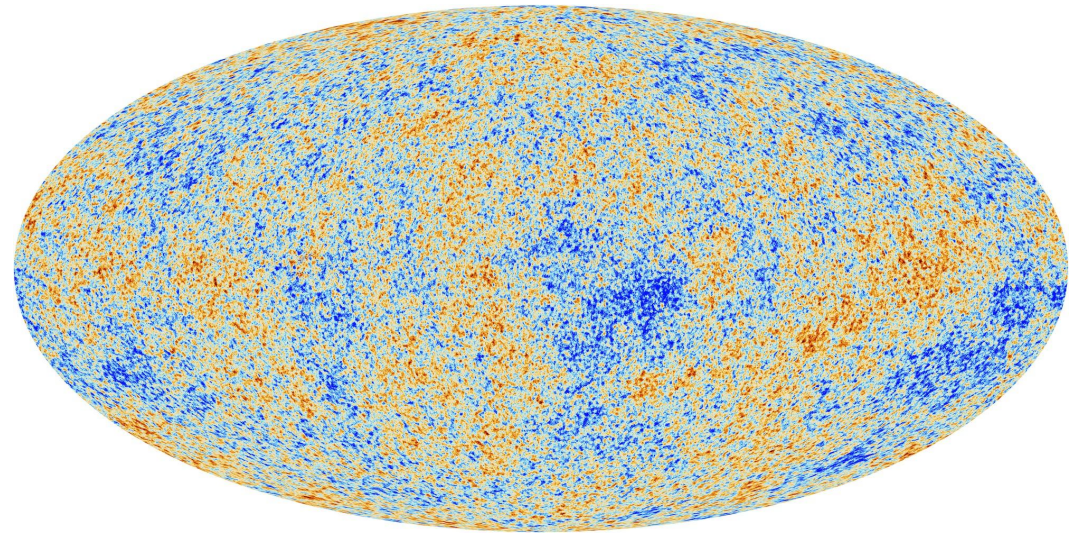


The Cosmic Microwave Background (CMB)

The CMB traces the conditions of the universe at the time when atoms first began to form.

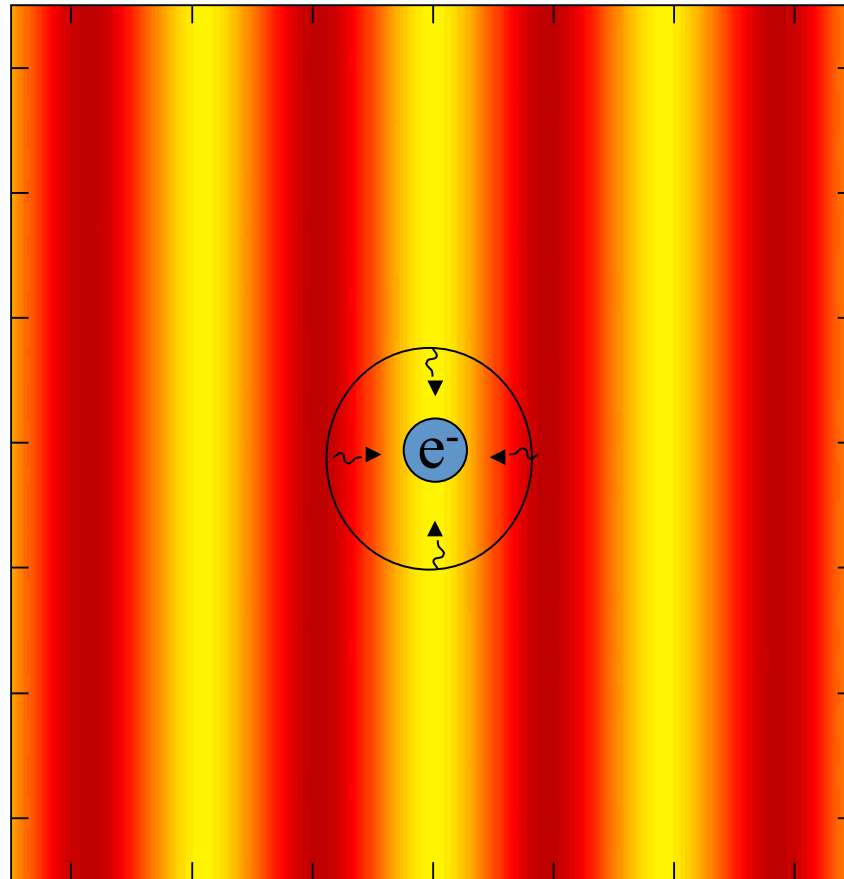
Precision measurements of the CMB temperature have provided a wealth of cosmological information consistent with the inflationary paradigm.

However, any imprint of the inflationary gravitational waves have so far eluded detection in the CMB.



Planck Collaboration & ESA

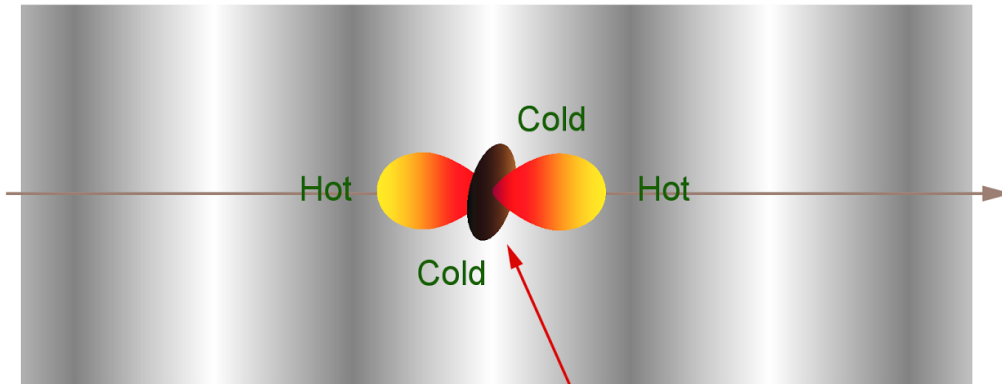
CMB polarization: arises at last scattering from local radiation quadrupole



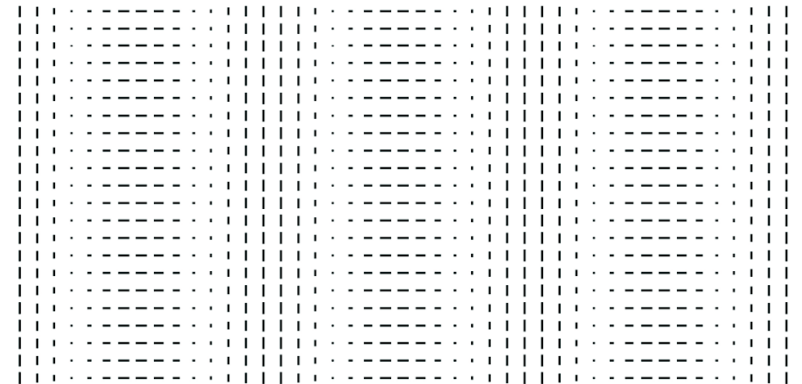
From Thomson scattering wherever there is ionized gas and quadrupole anisotropy

CMB polarization

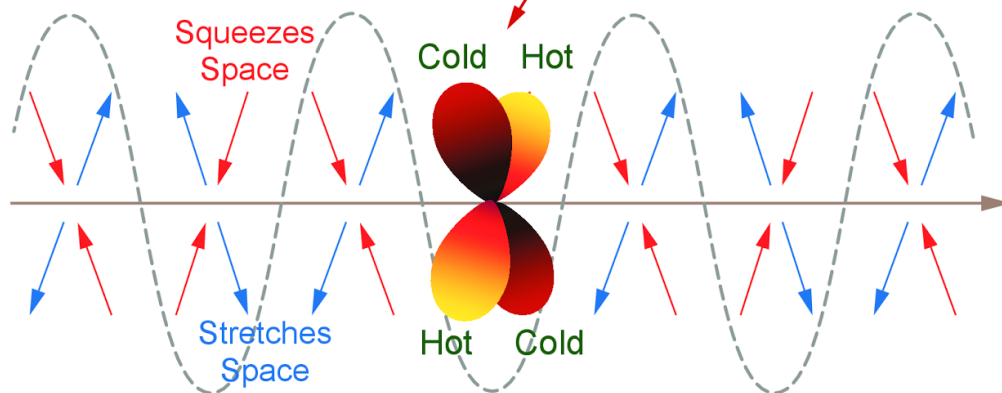
Density Wave



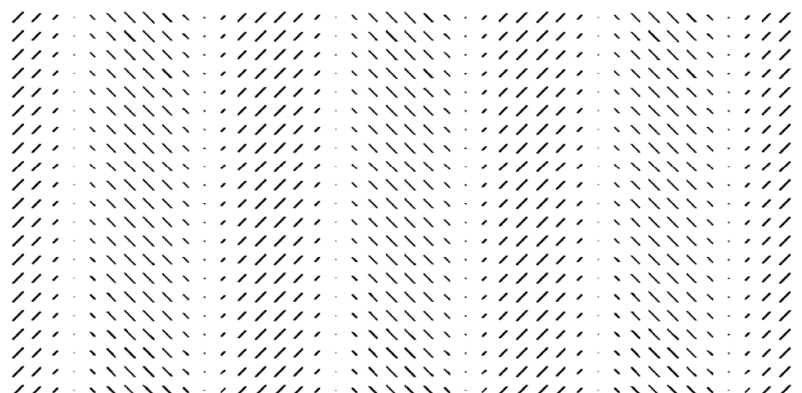
E-Mode Polarization Pattern



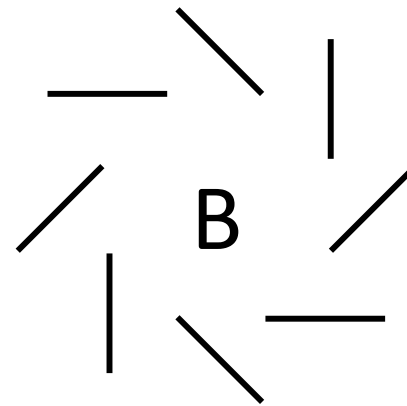
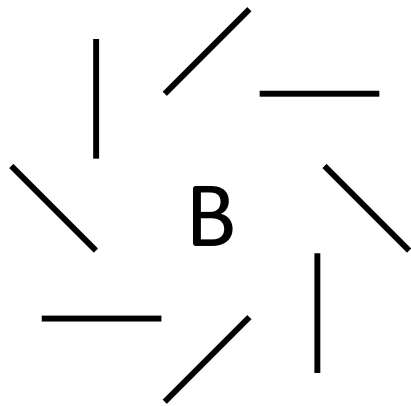
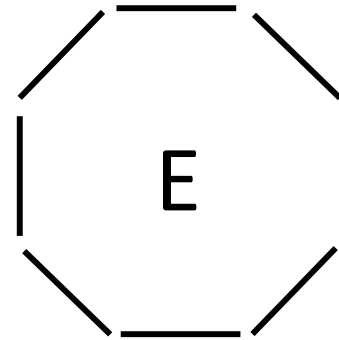
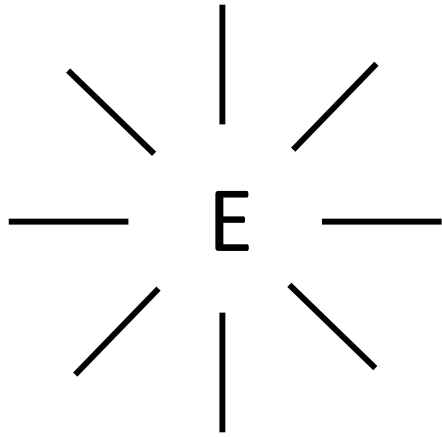
Gravitational Wave



B-Mode Polarization Pattern

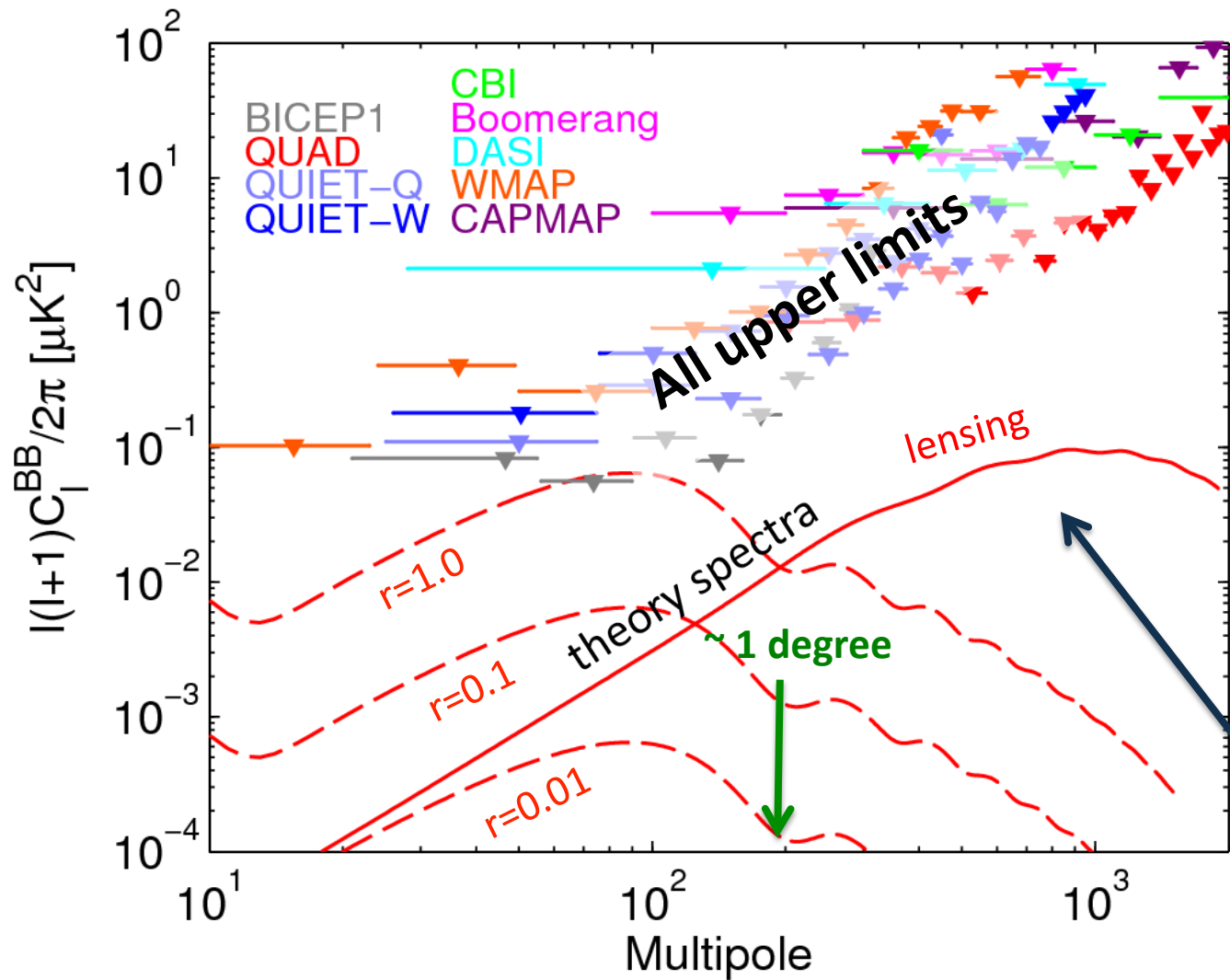


The signature of gravitational waves



Density fluctuations *cannot* make B-mode patterns

Search for B-modes



In simple inflationary gravitational wave models the

tensor-to-scalar ratio r

is the only parameter to the B-mode spectrum.

Until March 17 only upper limits

Best previous limit on r from BICEP1: $r < 0.7$ (95% CL)

Lensing deflects CMB photons, slightly mixing the dominant E-modes into B-modes -- dominant at high multipoles

B-modes from the ground

- Deep, Concentrated coverage
- Foreground avoidance (limited frequency)
- Systematic control with in-situ calibration
- Large detector count, rapid technology cycle
- Relentless observing & large number of null tests

→ powerful recipe for high-confidence initial discovery

BICEP2 Strategy: Unique Optics

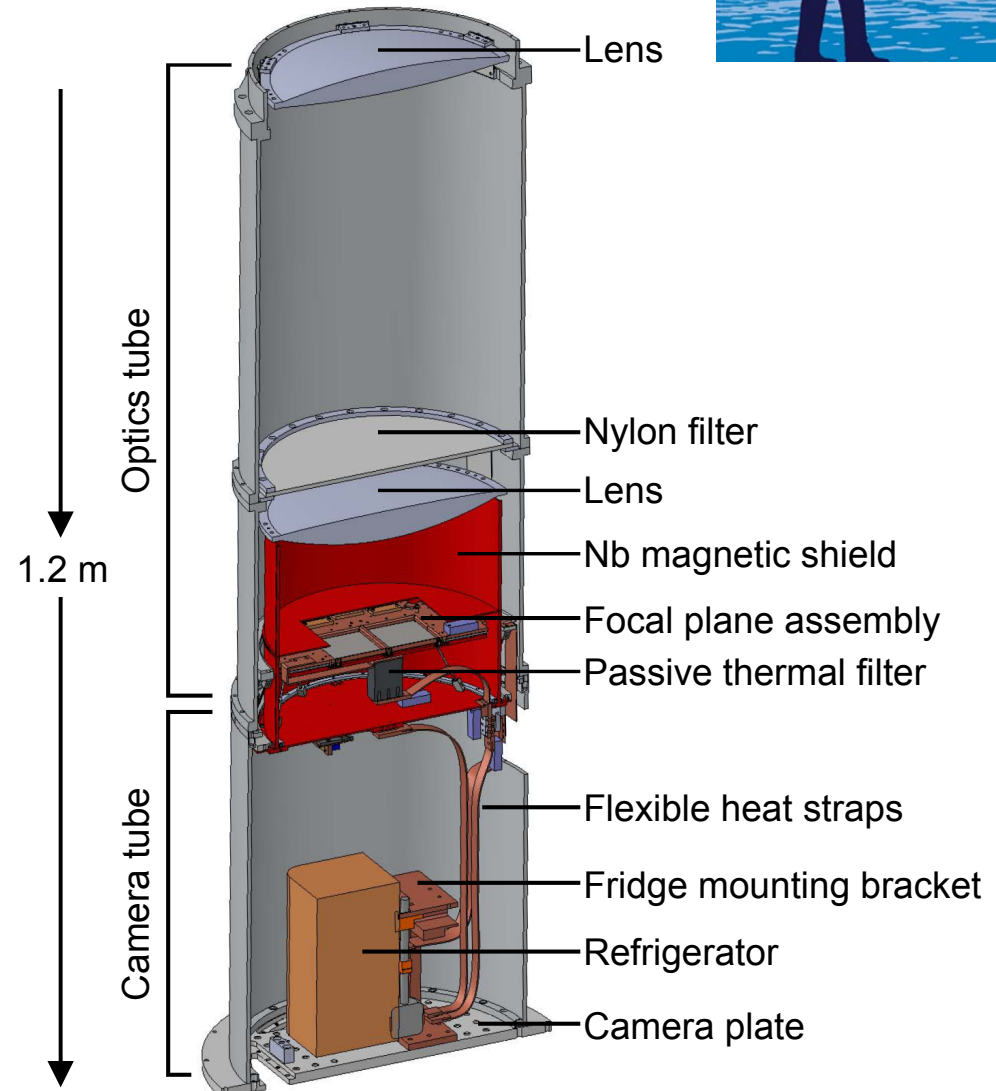


Telescope as compact as possible while still having the angular resolution to observe degree-scale features.

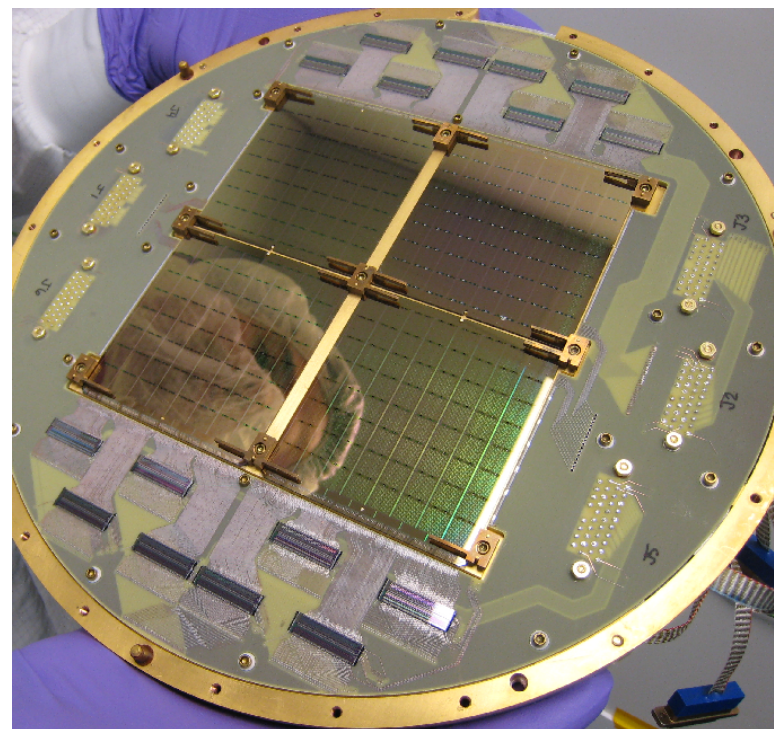
On-axis, refractive optics allow the entire telescope to rotate around boresight for polarization modulation.

Liquid helium cools the optical elements to 4.2 K.

A 3-stage helium sorption refrigerator further cools the detectors to 0.27 K.



BICEP2 Strategy: Revolutionary detectors

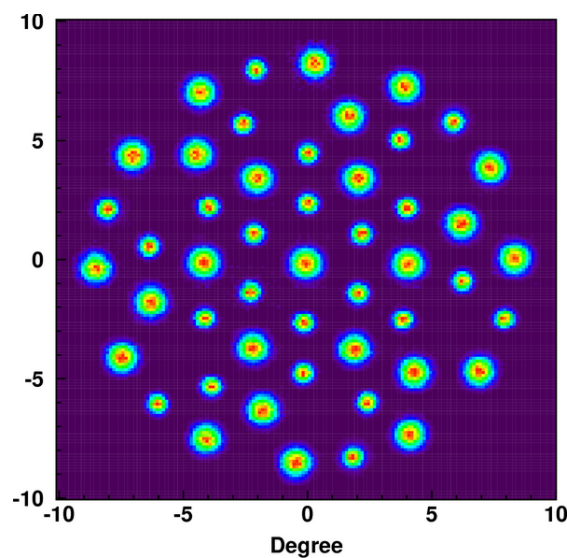


JPL : antenna-coupled TES arrays

BICEP1

48

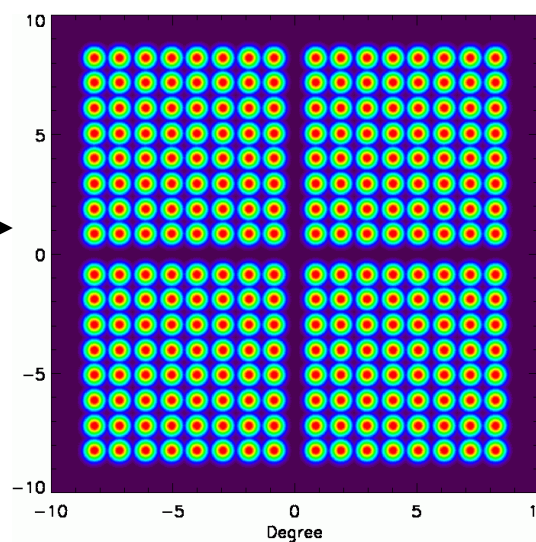
150 GHz
detectors



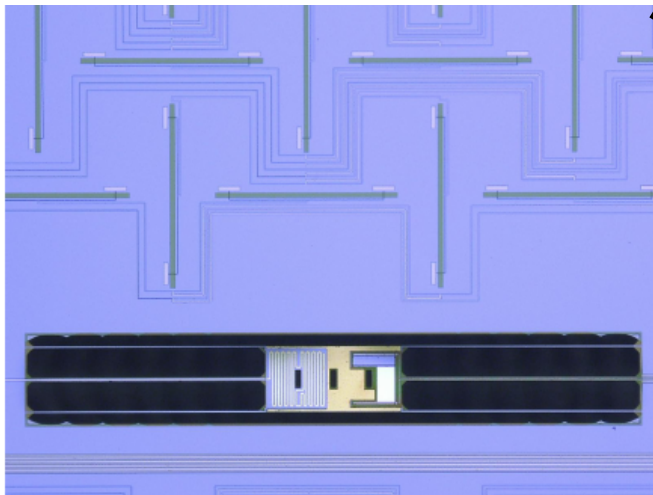
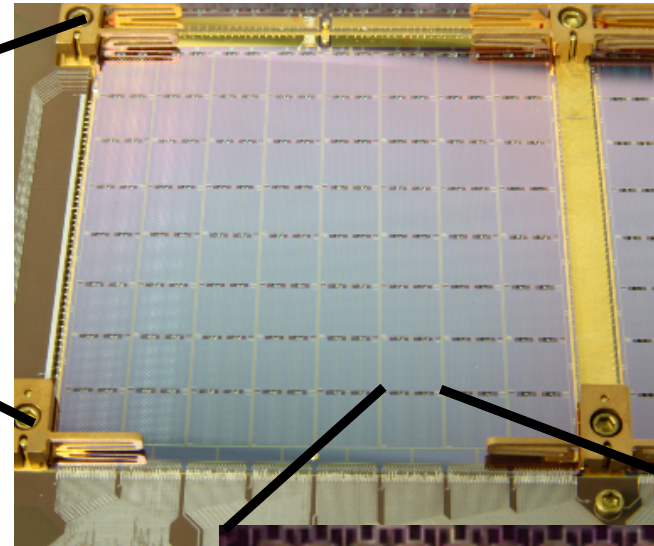
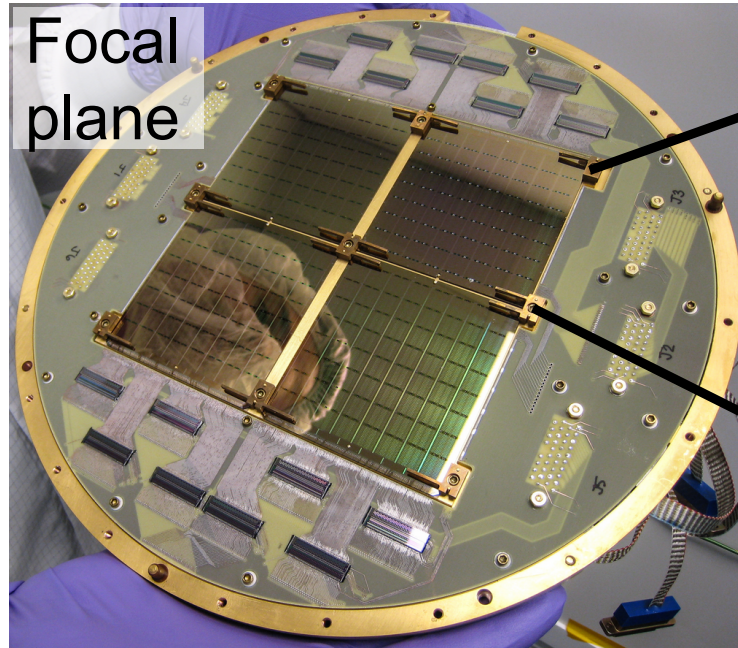
BICEP2

512

150 GHz
detectors



Mass-produced superconducting detectors

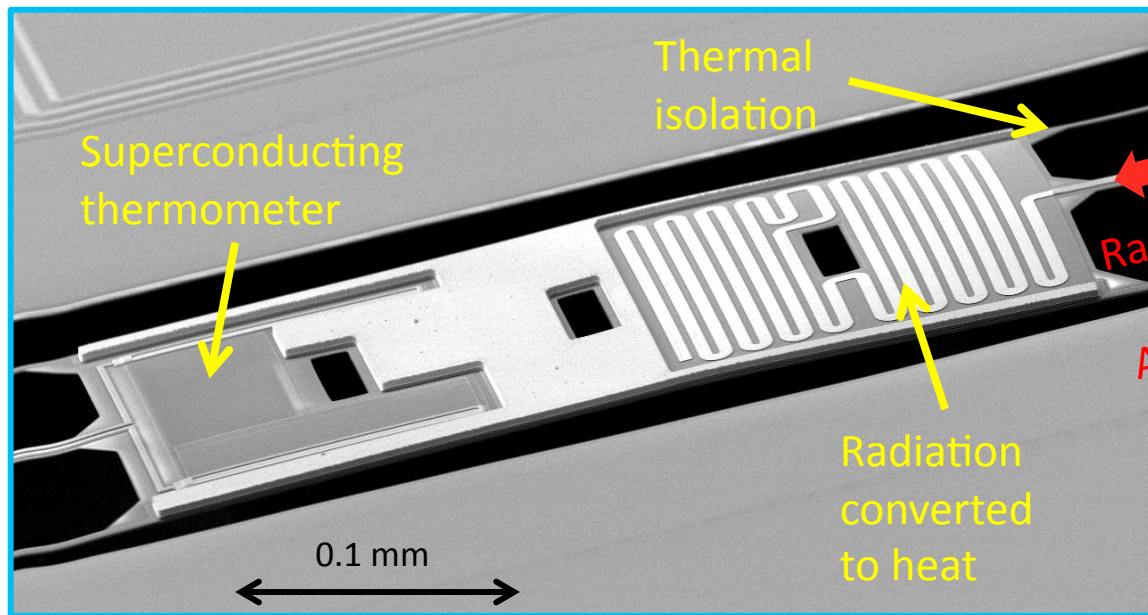


Slot antennas

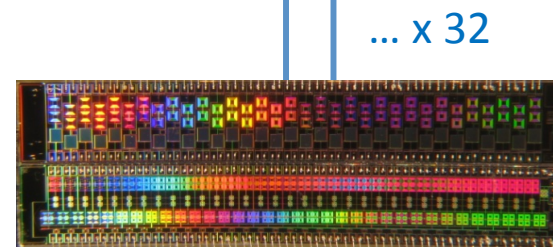
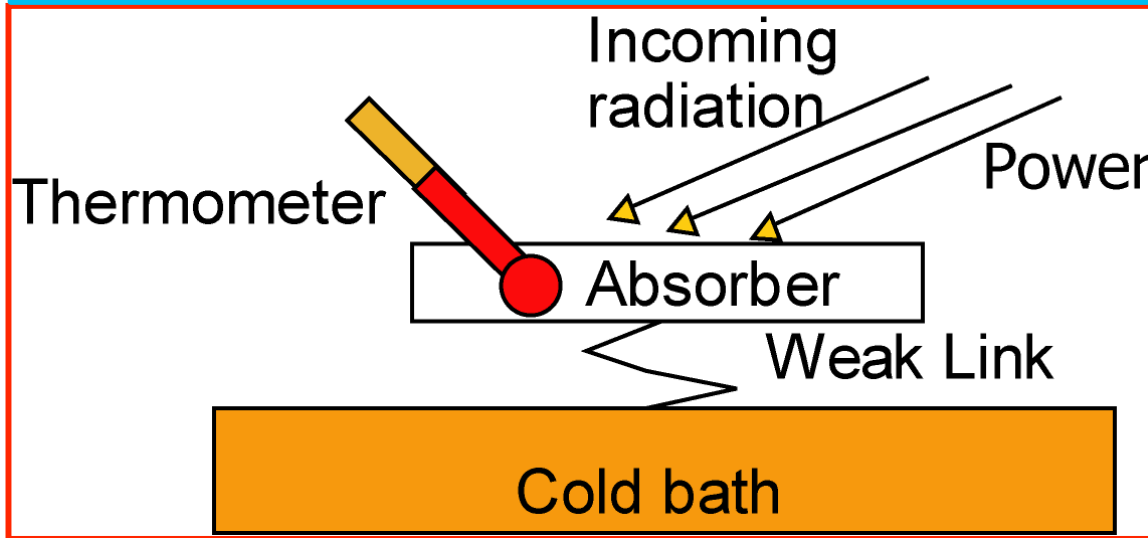
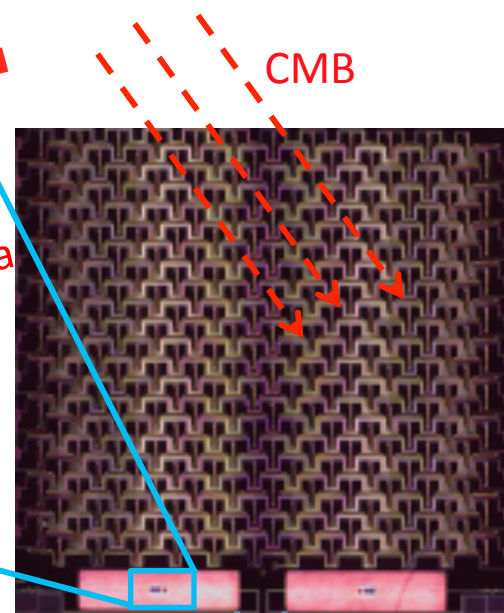
Transition edge sensor

Detecting CMB Radiation

BICEP2 Detector: Transition-Edge Sensor



Printed Antenna Gathers CMB Light



SQUIDs Amplify and Multiplex Signals

SQUIDs developed at NIST

Sensors cooled to 0.25 K to reduce thermal noise

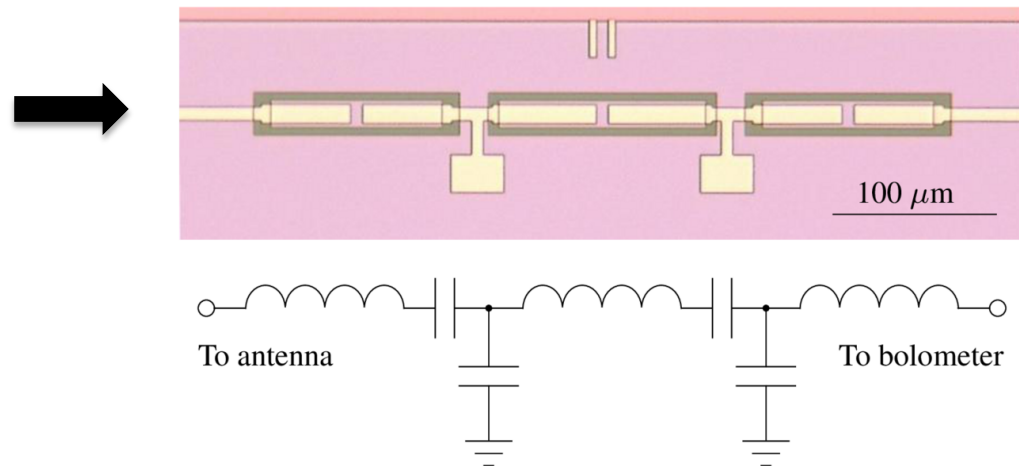
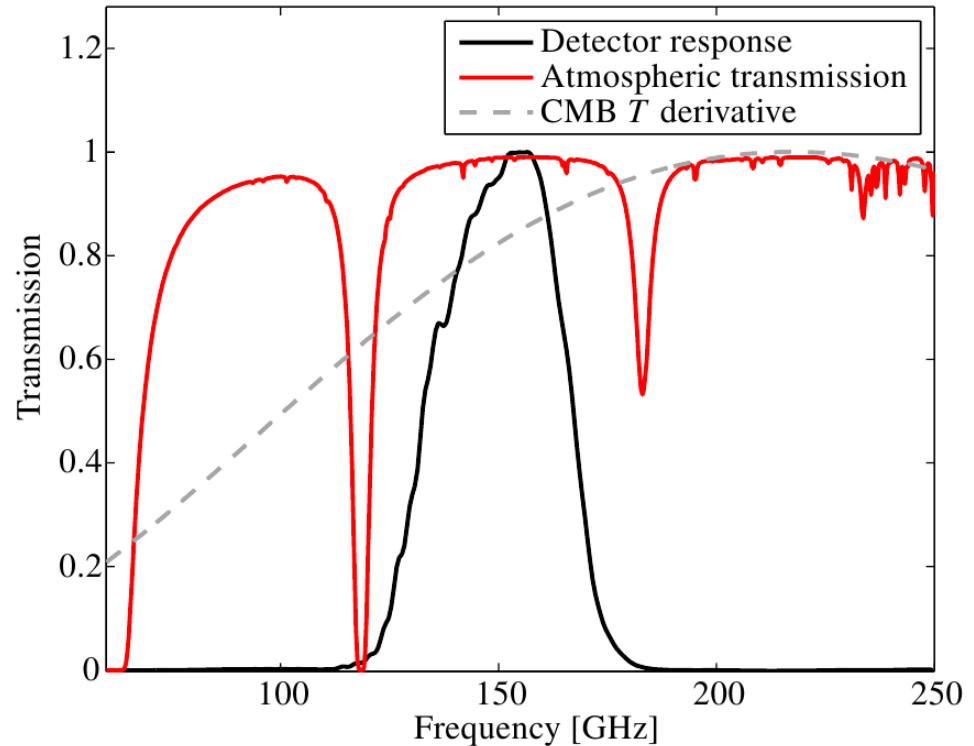
BICEP2 Frequency Response

The dry South Pole atmosphere provides excellent observing conditions most of the year.

The 28% fractional bandwidth fits within an atmospheric transmission window straddled by oxygen and water lines.

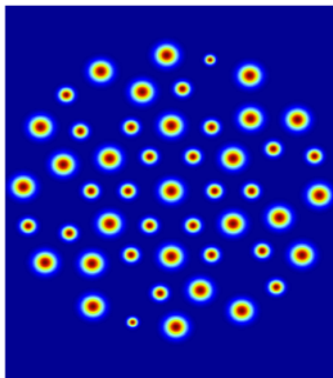
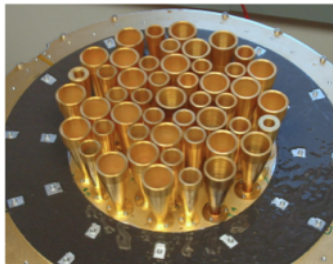
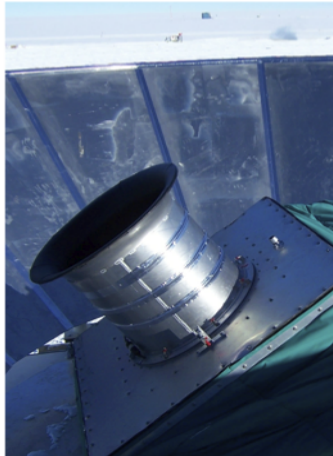
In this window, the atmosphere is transparent to microwaves.

The detector passband is defined by a filter printed directly onto the focal plane wafers.



Sensitivity through detector count increase

BICEP (2006–2008)



-5 0 5
Longitude (degrees)

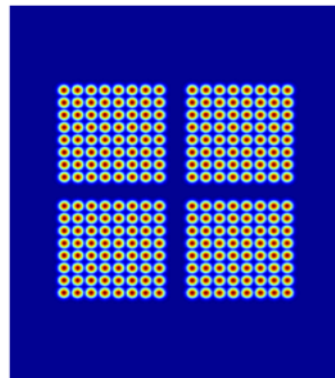
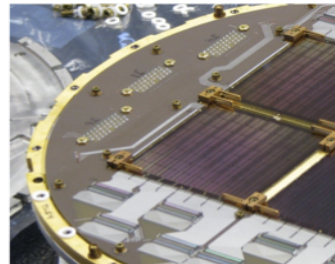
98 NTDs (95/150 GHz)

0.93°/0.60° FWHM

18° FOV

44 m² deg² AG

BICEP2 (2010–2012)



-5 0 5
Longitude (degrees)

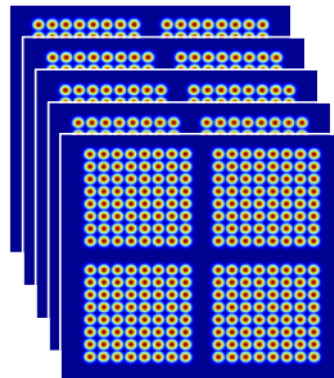
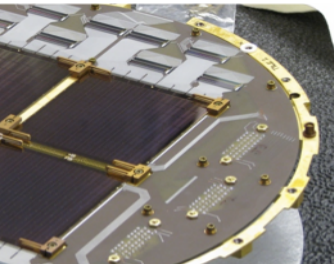
512 TESs (150 GHz)

0.52° FWHM

17° FOV

44 m² deg² AG

Keck Array (2011–2016)



-5 0 5
Longitude (degrees)

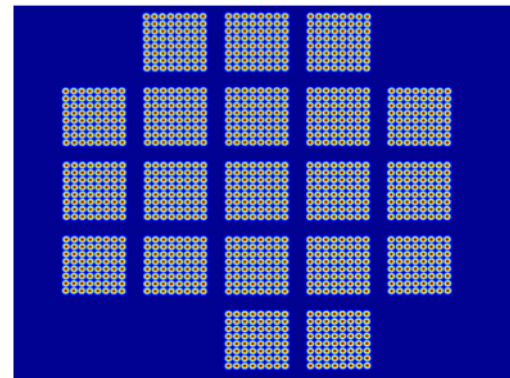
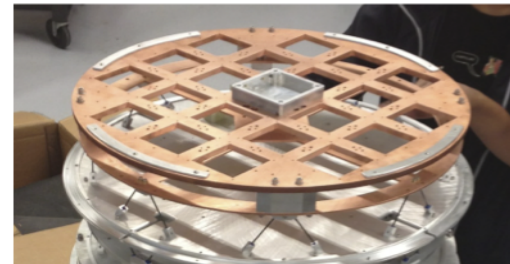
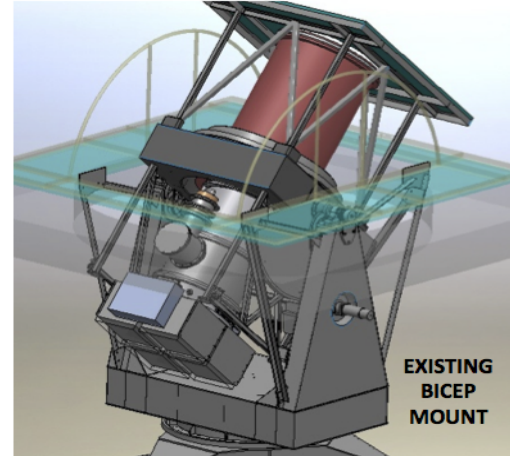
2560 TESs (150 GHz)

0.52° FWHM

17° FOV

333 m² deg² AG

BICEP3 (2014-)



-10 -5 0 5 10
Longitude (degrees)

2560 TESs (95 GHz)

0.37° FWHM

26° FOV

503 m² deg² AG optical throughput

EXISTING
BICEP
MOUNT

BICEP2 Strategy: the South Pole



South Pole CMB telescopes



**NSF's South Pole Station:
A popular place with CMB Experimentalists!**

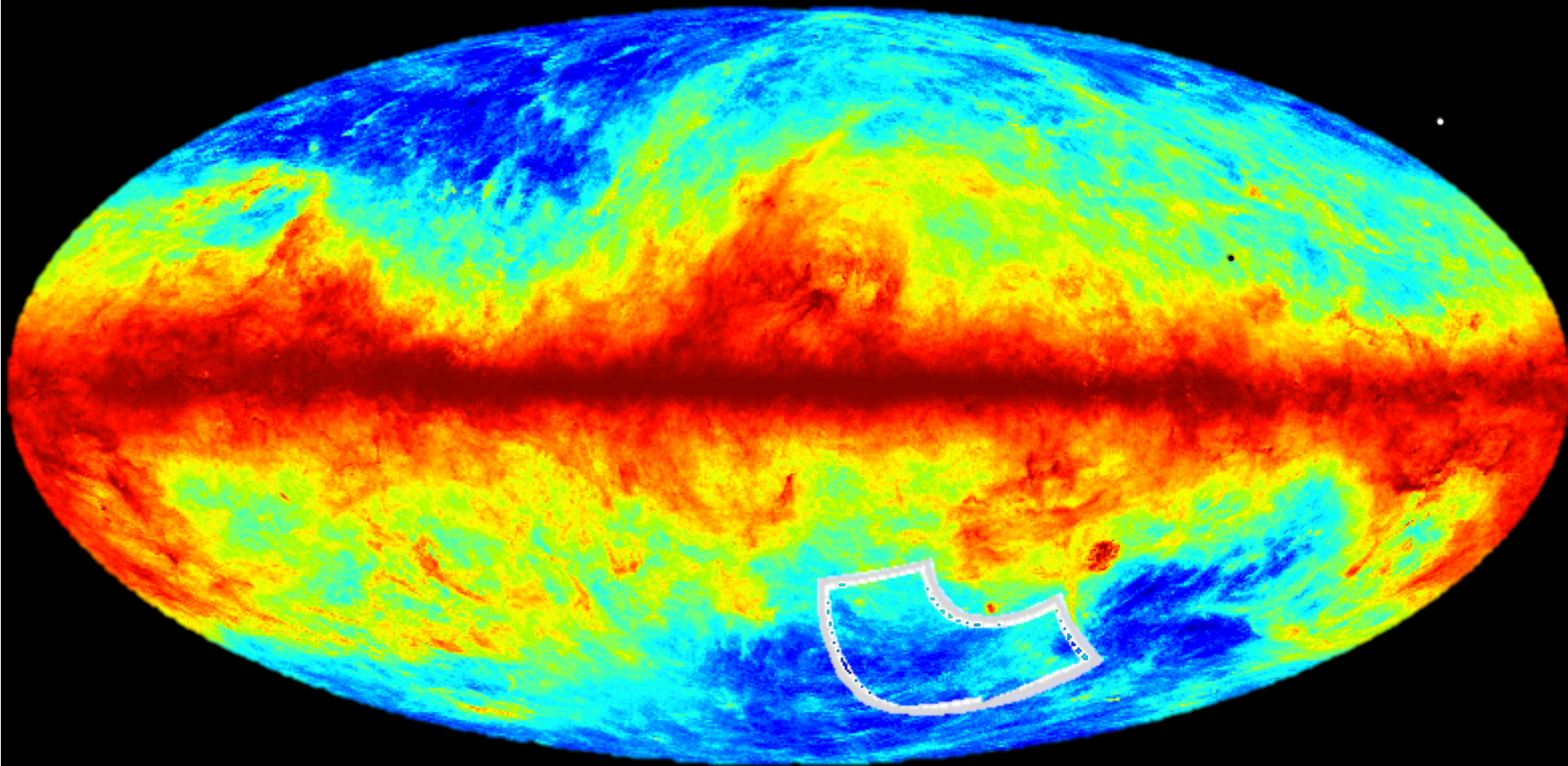
**Super dry atmosphere and 24h coverage of "Southern Hole".
Also power, LHe, LN₂, 200 GB/day, 3 square meals,...**



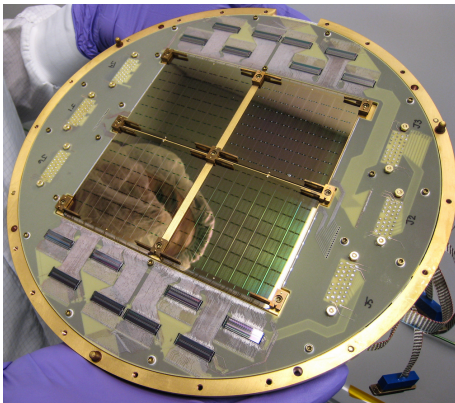
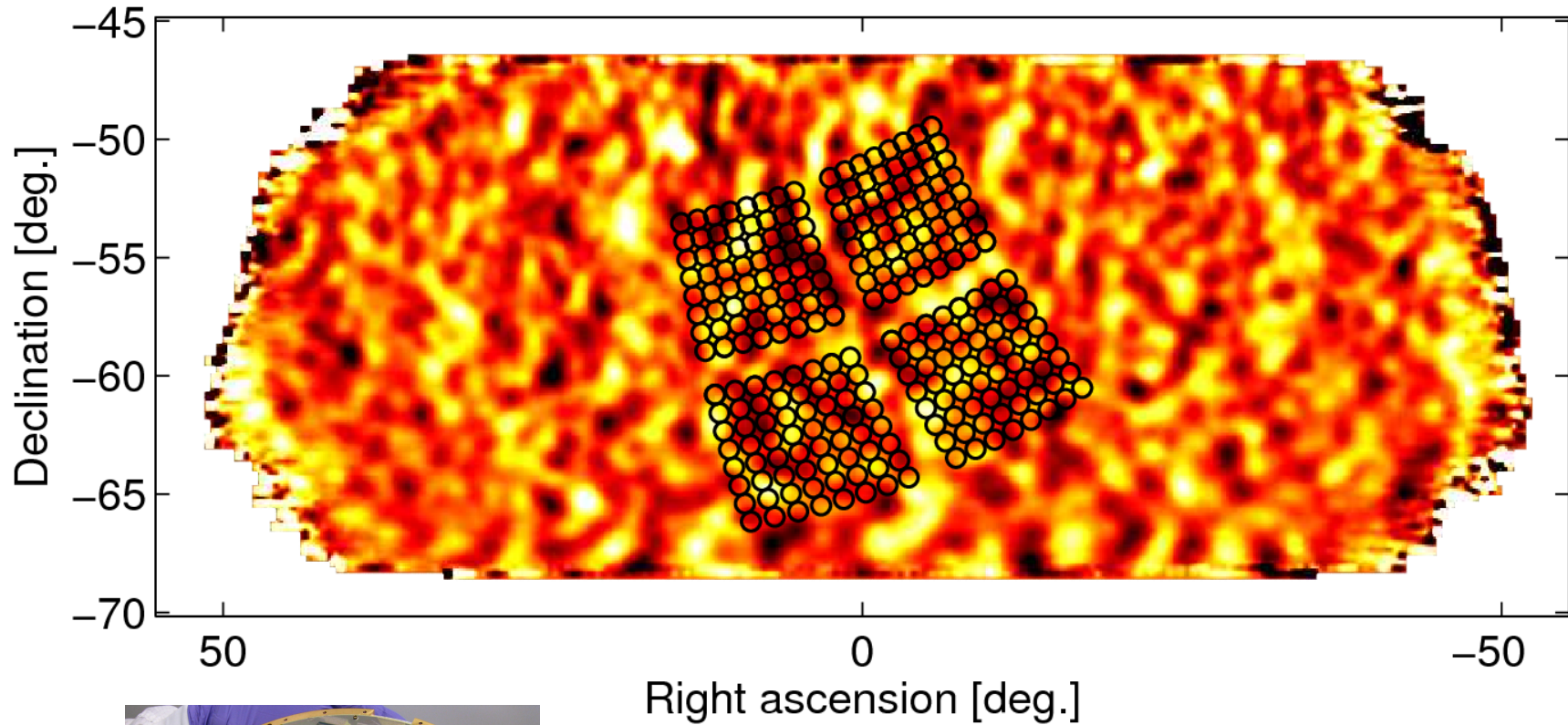
photo: Keith Vanderlinde

BICEP2 Strategy: The Best Field

- Observe the “Southern Hole” at 150 GHz
- a region of the sky exceptionally free of dust and radio emission from our galaxy



BICEP2 on the Sky



Projection of the BICEP2 focal plane on the sky

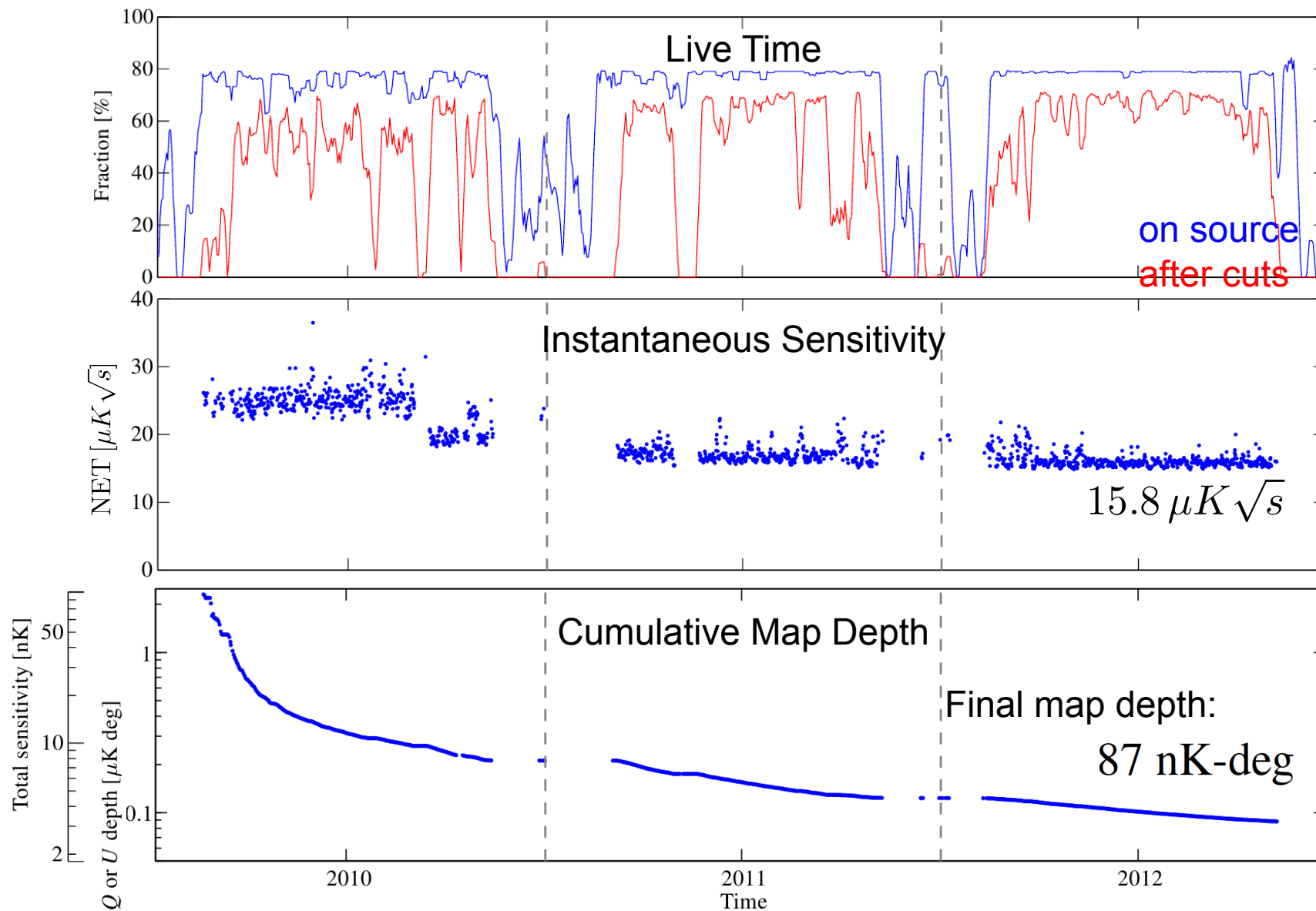
The focal plane is 20 degrees across

Background is the CMB temperature map as measured with BICEP2

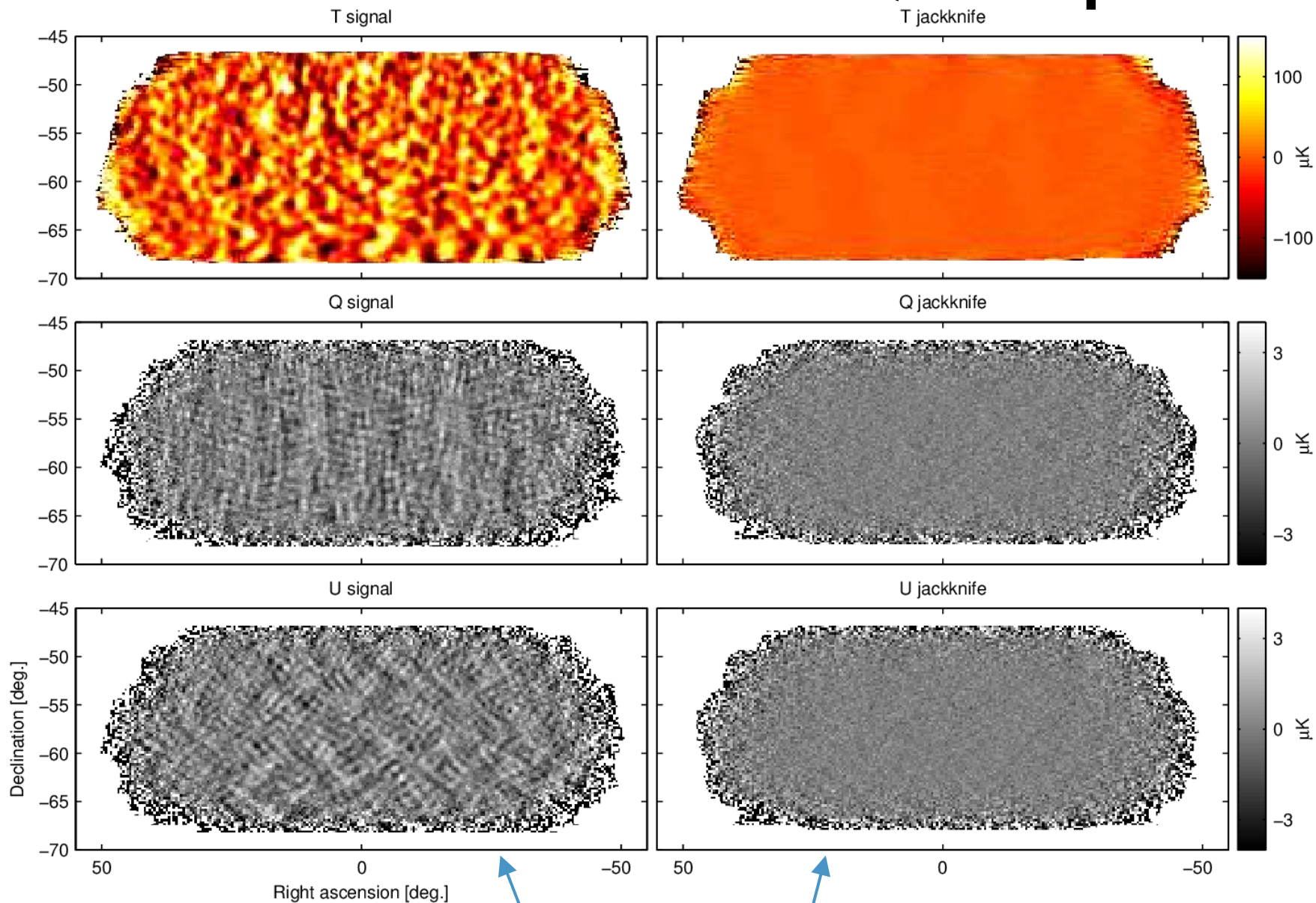
South Pole: “Relentless Observing”



BICEP2 3-year Data Set



BICEP2 T and Stokes Q/U Maps

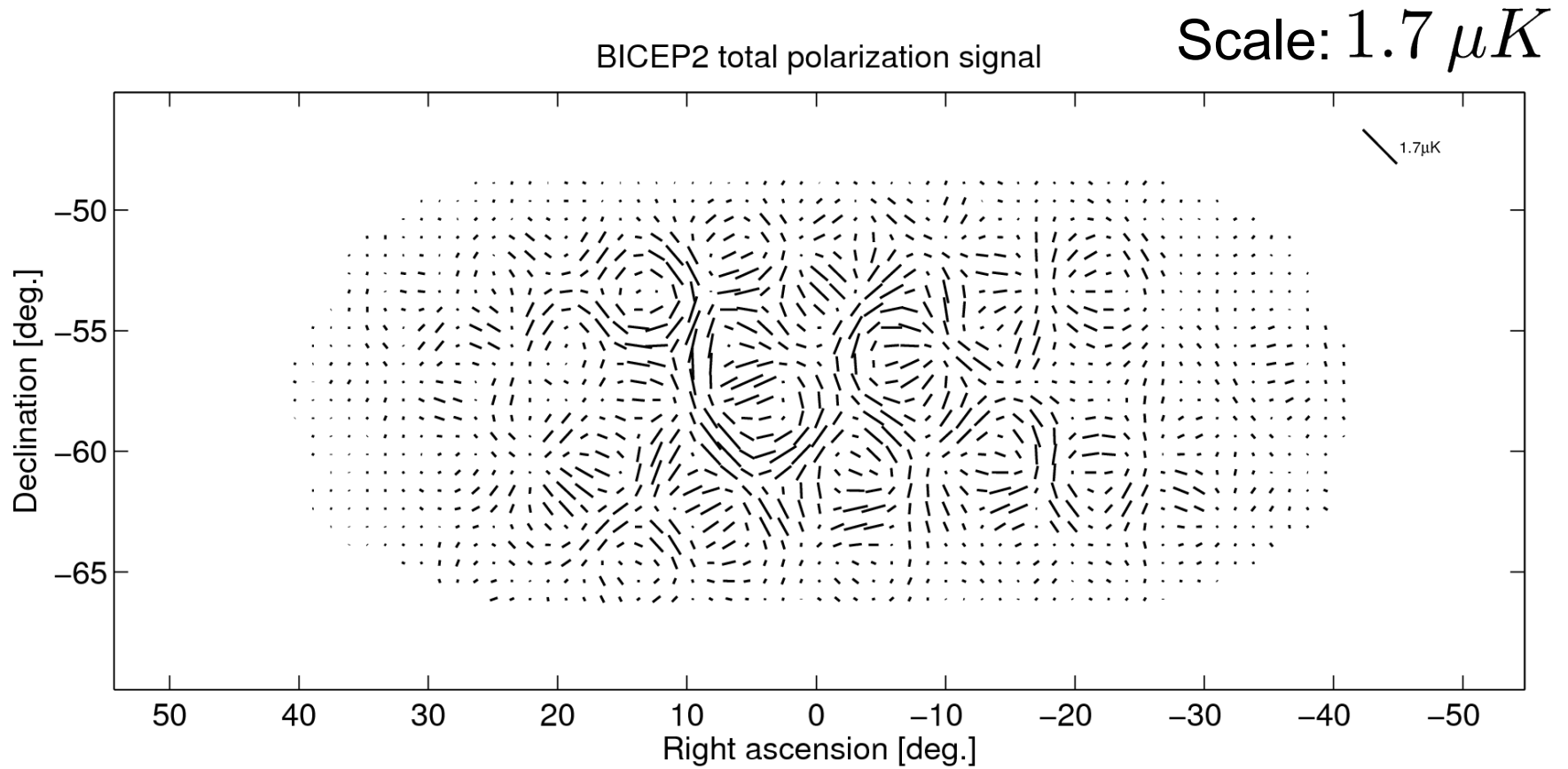


Angiola Orlando for The Bicep2 Collaboration

Signal Maps

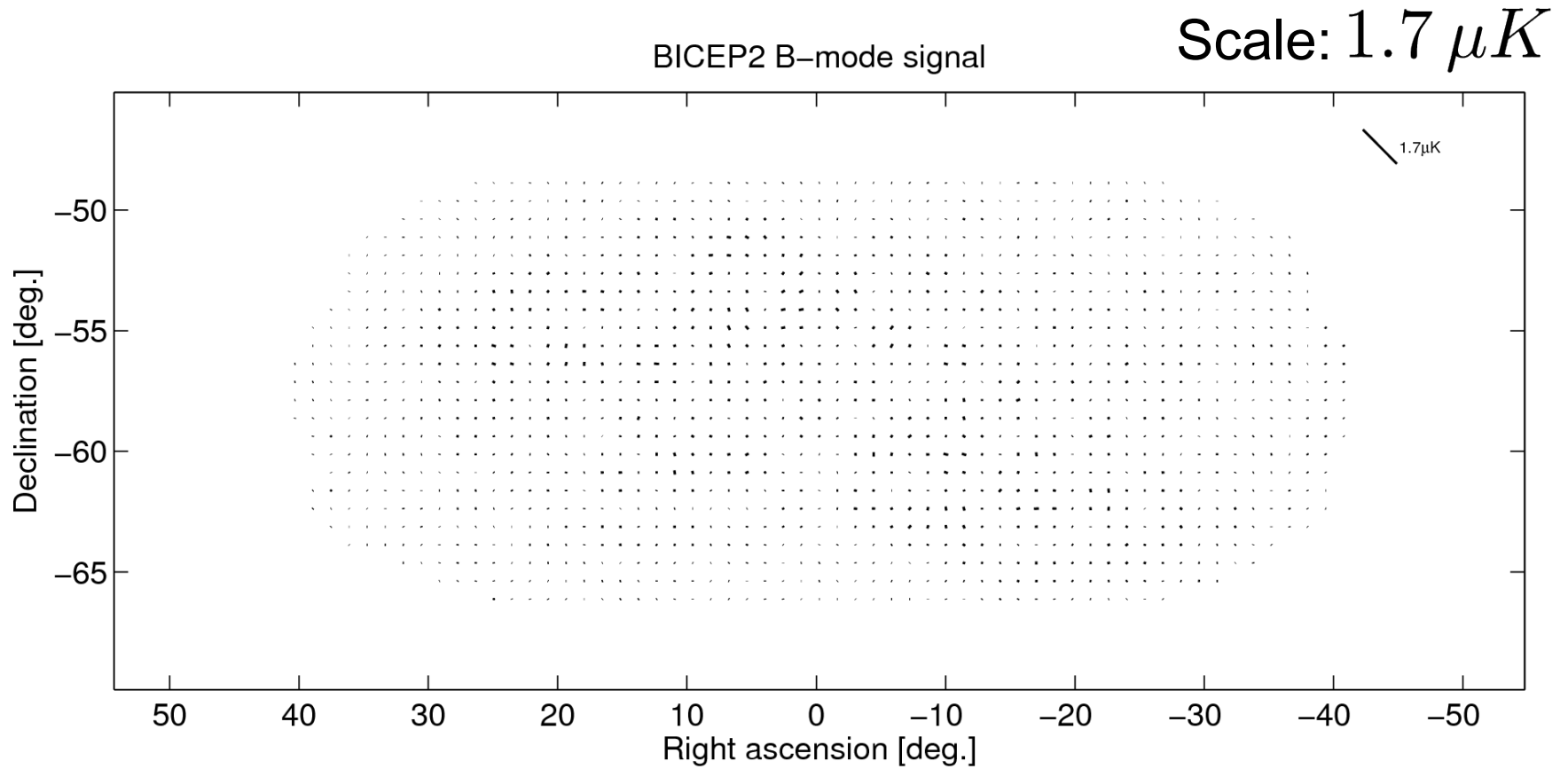
Difference ("Jackknife") Maps

Total Polarization



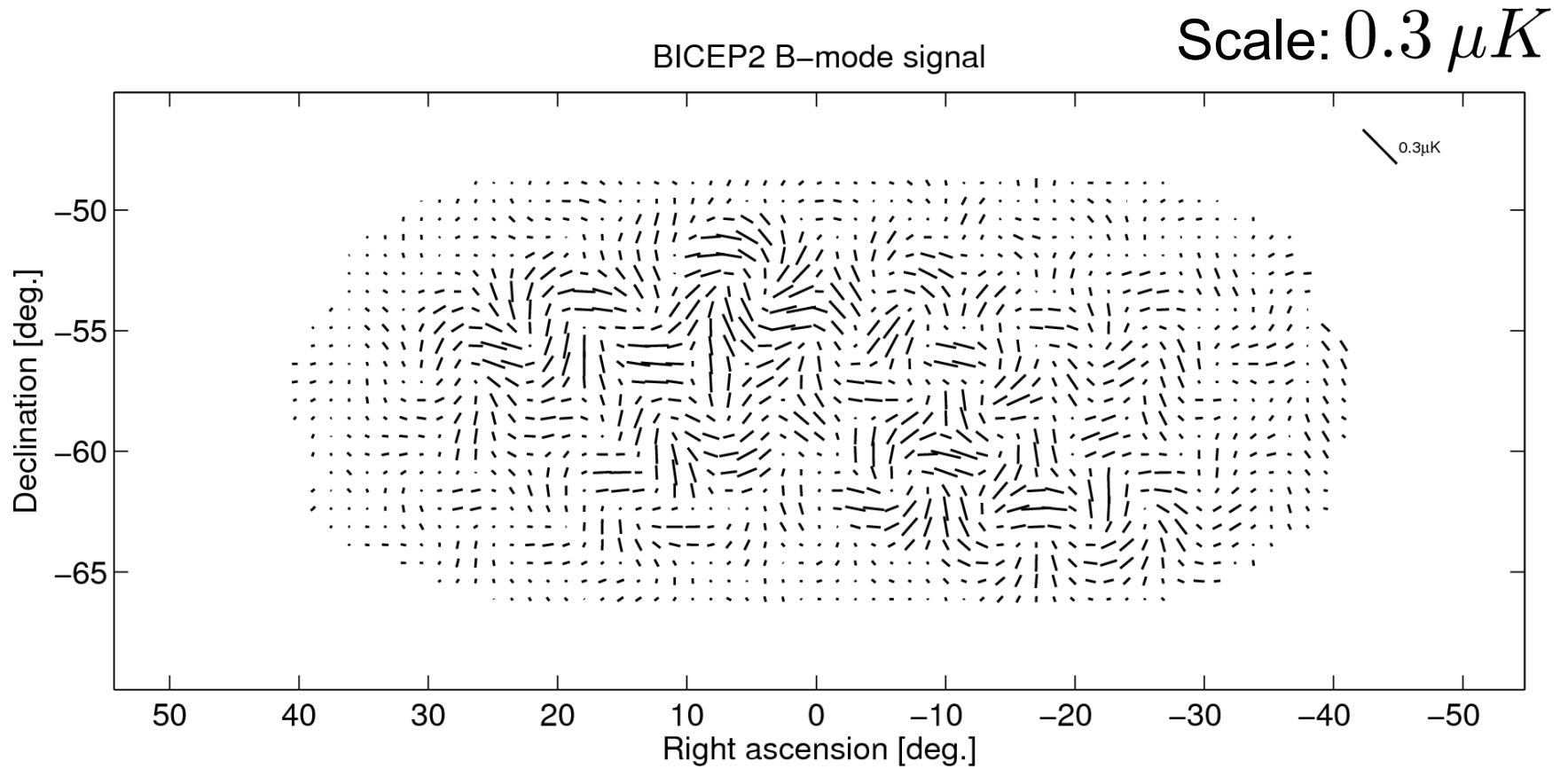
B-modes of $r=0.1$ contribute $\sim 1/10$ of the total polarization amplitude at $l=100$

B-mode Contribution



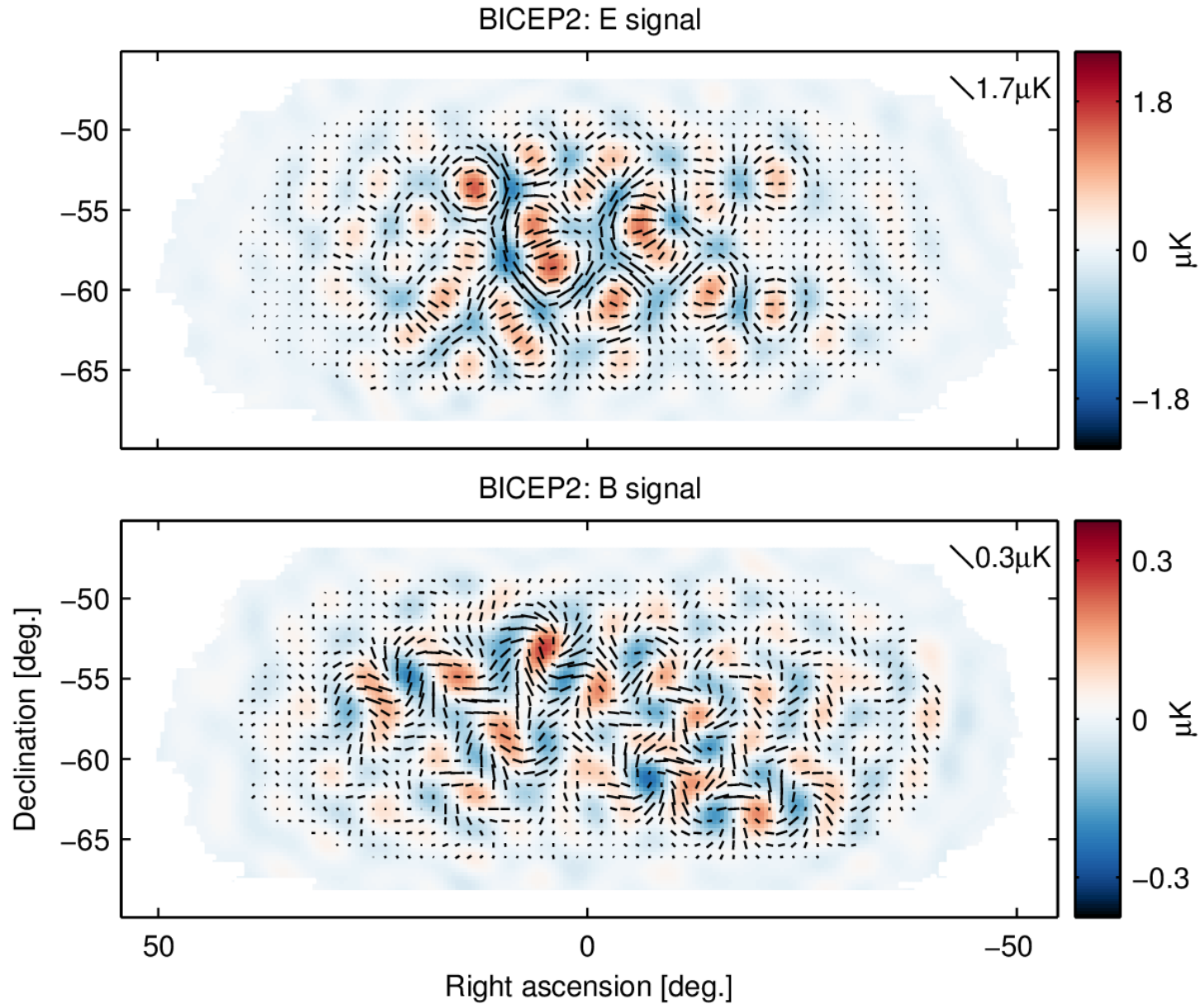
B-modes of $r=0.1$ contribute $\sim 1/10$ of the total polarization amplitude at $l=100$

B-mode Contribution

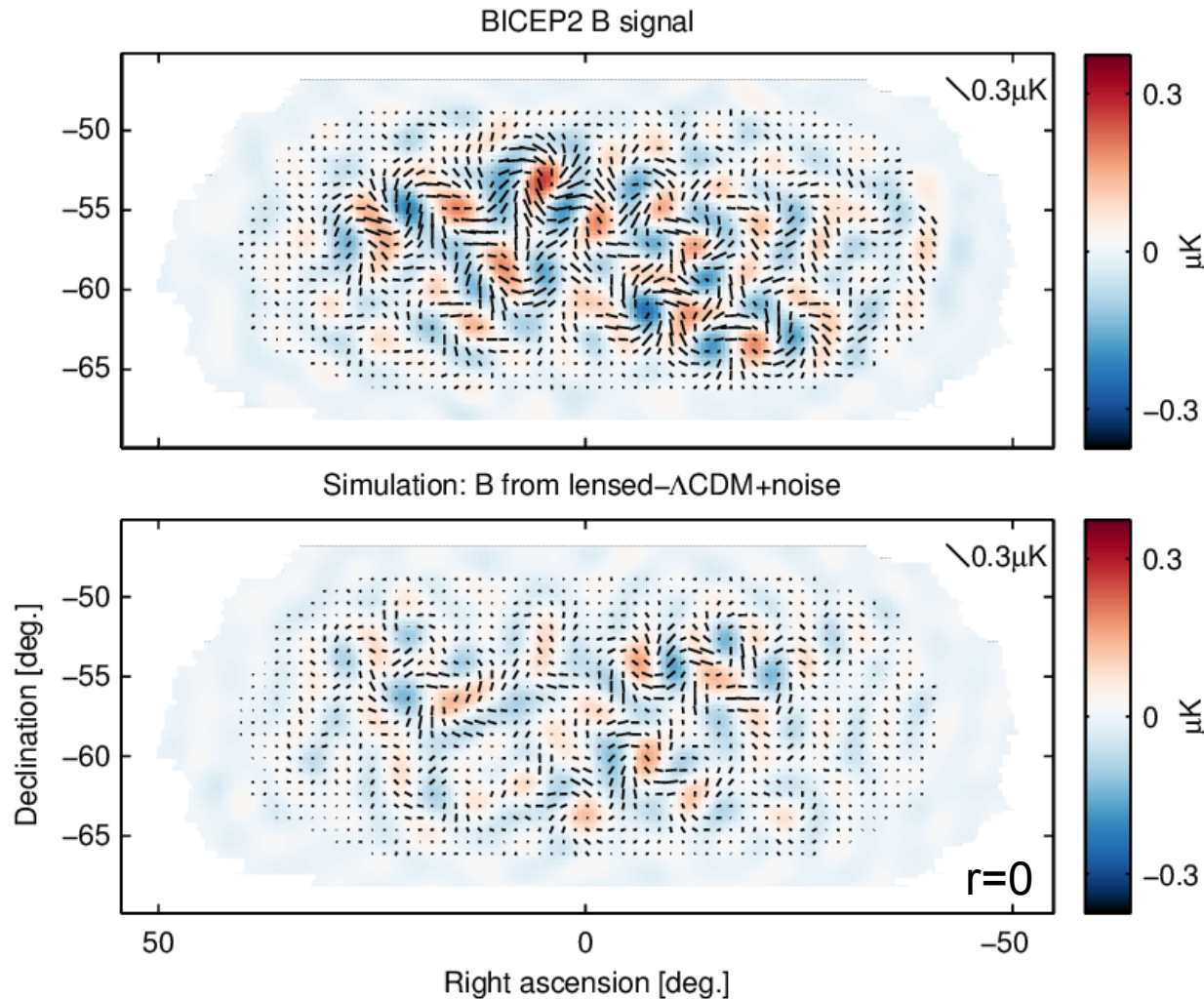


Zoom in by factor 6 – see “swirly” B-mode

BICEP2 E- and B-mode Maps



B-mode Map vs. Simulation



Simulation pipeline:

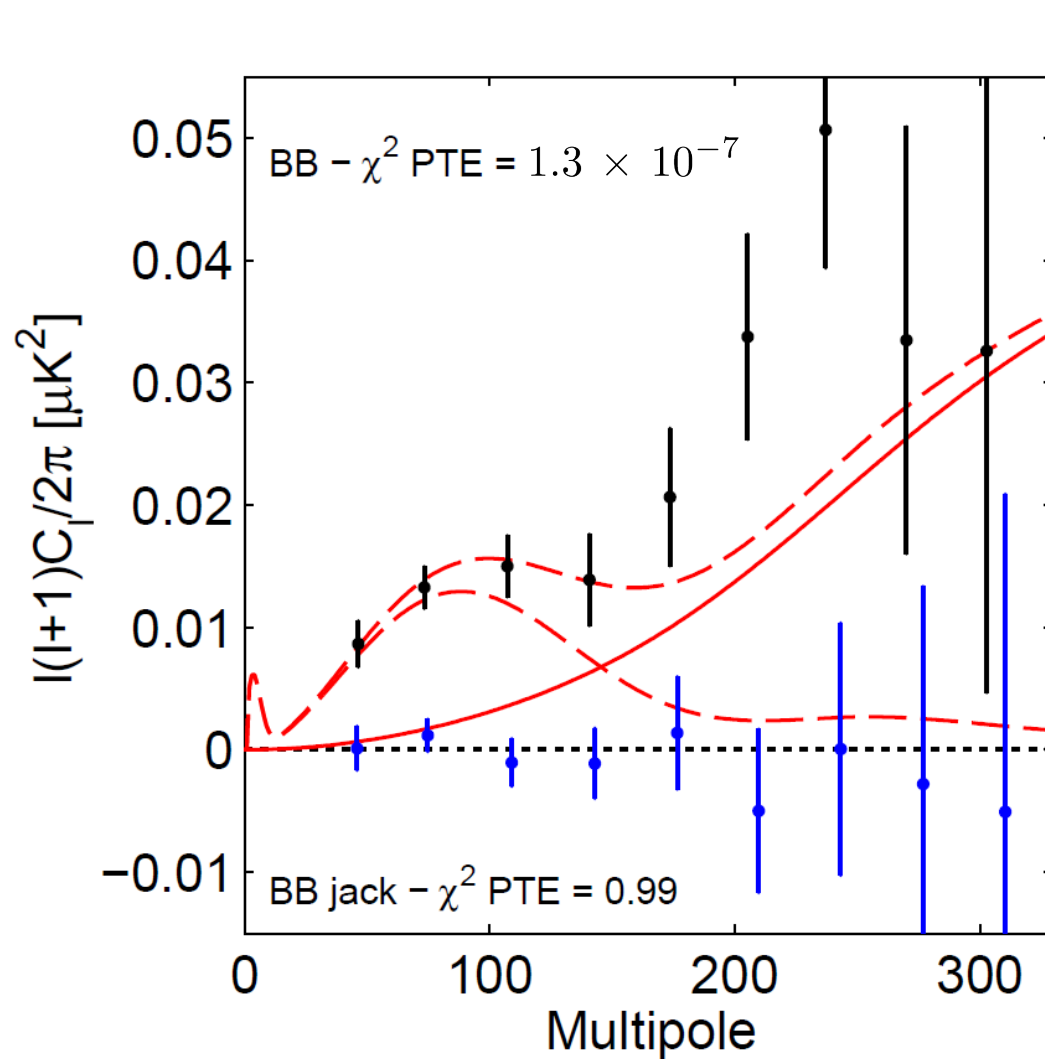
generate realizations of the full observation and all filtering operations.

Compare real data to 500 lensed- Λ CDM+noise simulations each at various levels of r .

We perform various filtering operations: use the sims to correct for these.

Also use the sims to derive the final uncertainties (error bars)

BICEP2 B-mode Power Spectrum



—●— B-mode power spectrum

—●— temporal split jackknife

— lensed- Λ CDM

- - - r=0.2

B-mode power spectrum estimated from Q&U maps, including map based “purification” to avoid E→B mixing

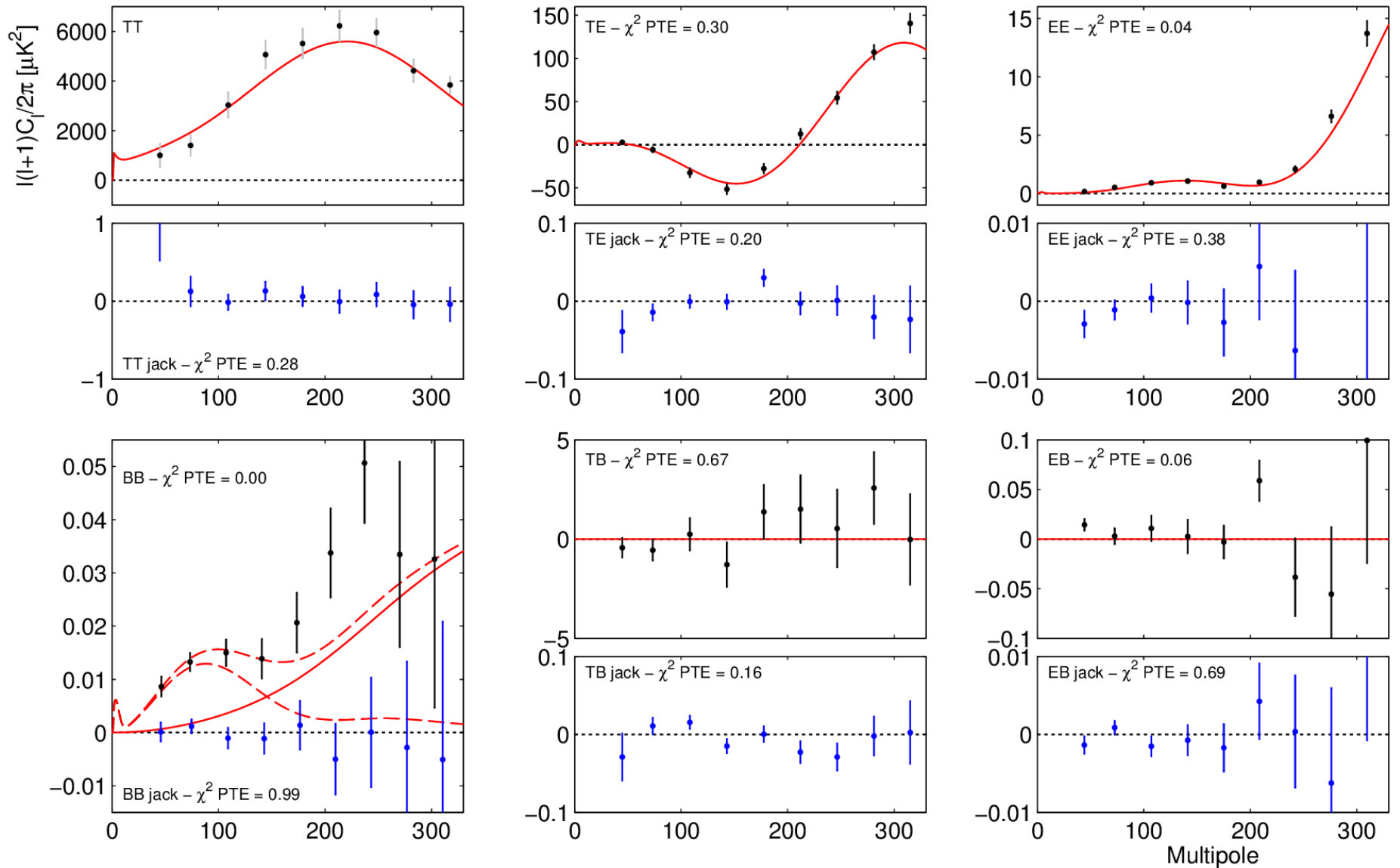
Consistent with lensing expectation at higher l .

At low l excess over lensed- Λ CDM with high signal-to-noise.

For the hypothesis that the measured band powers come from lensed- Λ CDM we find:

| | |
|--------------|----------------------|
| χ^2 PTE | 1.3×10^{-7} |
| significance | 5.2σ |

Temperature and Polarization Power Spectra



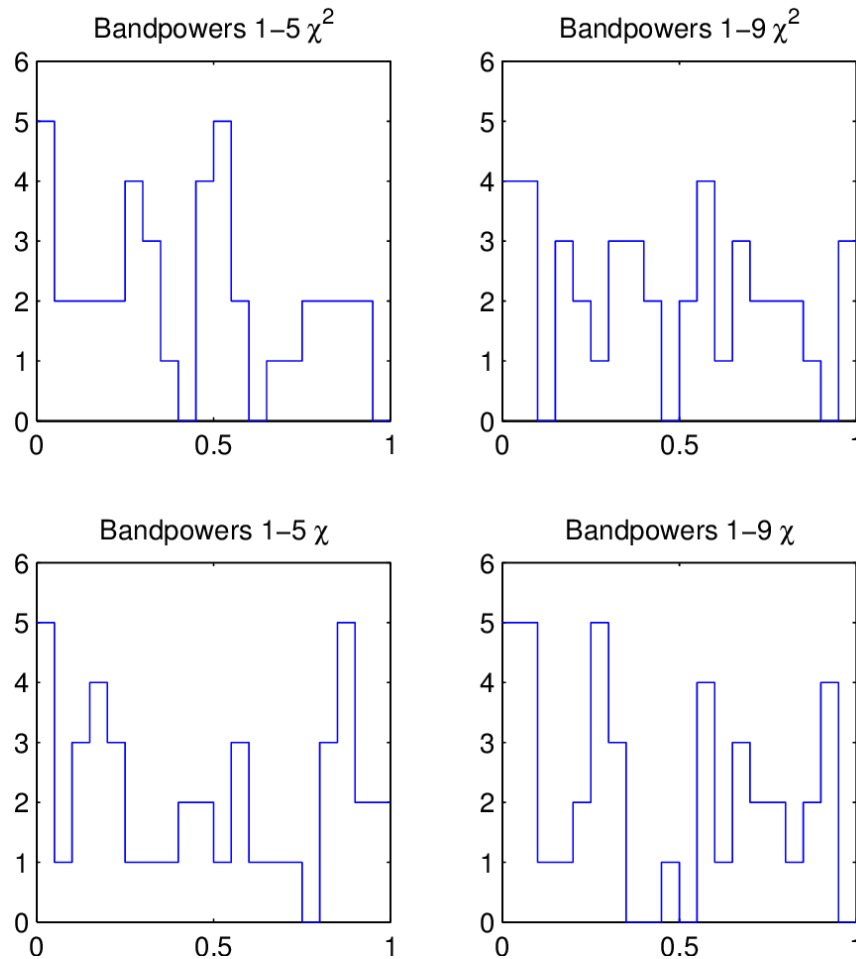
Check Systematics: Jackknives

TABLE 1
JACKKNIFE PTE VALUES FROM χ^2 AND χ (SUM-OF-DEVIATION)
TESTS

| Jackknife | Bandpowers 1-5 χ^2 | Bandpowers 1-9 χ^2 | Bandpowers 1-5 χ | Bandpowers 1-9 χ |
|-----------------------------------|----------------------------|----------------------------|--------------------------|--------------------------|
| Deck jackknife | | | | |
| EE | 0.046 | 0.030 | 0.164 | 0.299 |
| BB | 0.774 | 0.329 | 0.240 | 0.082 |
| EB | 0.337 | 0.643 | 0.204 | 0.267 |
| Scan Dir jackknife | | | | |
| EE | 0.483 | 0.762 | 0.978 | 0.938 |
| BB | 0.531 | 0.573 | 0.896 | 0.551 |
| EB | 0.898 | 0.806 | 0.725 | 0.890 |
| Tag Split jackknife | | | | |
| EE | 0.541 | 0.377 | 0.916 | 0.938 |
| BB | 0.902 | 0.992 | 0.449 | 0.585 |
| EB | 0.477 | 0.689 | 0.856 | 0.615 |
| Tile jackknife | | | | |
| EE | 0.004 | 0.010 | 0.000 | 0.002 |
| BB | 0.794 | 0.752 | 0.565 | 0.331 |
| EB | 0.172 | 0.419 | 0.962 | 0.790 |
| Phase jackknife | | | | |
| EE | 0.673 | 0.409 | 0.126 | 0.339 |
| BB | 0.591 | 0.739 | 0.842 | 0.944 |
| EB | 0.529 | 0.577 | 0.840 | 0.659 |
| Mux Col jackknife | | | | |
| EE | 0.812 | 0.587 | 0.196 | 0.204 |
| BB | 0.826 | 0.972 | 0.293 | 0.283 |
| EB | 0.866 | 0.968 | 0.876 | 0.697 |
| Alt Deck jackknife | | | | |
| EE | 0.004 | 0.004 | 0.070 | 0.236 |
| BB | 0.397 | 0.176 | 0.381 | 0.086 |
| EB | 0.150 | 0.060 | 0.170 | 0.291 |
| Mux Row jackknife | | | | |
| EE | 0.052 | 0.178 | 0.653 | 0.739 |
| BB | 0.345 | 0.361 | 0.032 | 0.008 |
| EB | 0.529 | 0.226 | 0.024 | 0.048 |
| Tile/Deck jackknife | | | | |
| EE | 0.048 | 0.088 | 0.144 | 0.132 |
| BB | 0.908 | 0.840 | 0.629 | 0.269 |
| EB | 0.050 | 0.154 | 0.591 | 0.591 |
| Focal Plane inner/outer jackknife | | | | |
| EE | 0.230 | 0.597 | 0.022 | 0.090 |
| BB | 0.216 | 0.531 | 0.046 | 0.092 |
| EB | 0.036 | 0.042 | 0.850 | 0.838 |
| Tile top/bottom jackknife | | | | |
| EE | 0.289 | 0.347 | 0.459 | 0.599 |
| BB | 0.293 | 0.236 | 0.154 | 0.028 |
| EB | 0.545 | 0.683 | 0.902 | 0.932 |
| Tile inner/outer jackknife | | | | |
| EE | 0.727 | 0.533 | 0.128 | 0.485 |
| BB | 0.255 | 0.086 | 0.421 | 0.036 |
| EB | 0.465 | 0.737 | 0.208 | 0.168 |
| Moon jackknife | | | | |
| EE | 0.499 | 0.689 | 0.481 | 0.679 |
| BB | 0.144 | 0.287 | 0.898 | 0.858 |
| EB | 0.289 | 0.359 | 0.531 | 0.307 |
| A/B offset best/worst | | | | |
| EE | 0.317 | 0.311 | 0.868 | 0.709 |
| BB | 0.114 | 0.064 | 0.307 | 0.094 |
| EB | 0.589 | 0.872 | 0.599 | 0.790 |

14 jackknife tests applied to 3 spectra, 4 statistics

All 4 jackknife statistics have uniform probability to exceed (PTE) distributions:



Check Systematics: Jackknives

TABLE 1
JACKKNIFE PTE VALUES FROM χ^2 AND χ (SUM-OF-DEVIATION)
TESTS

| Jackknife | Bandpowers 1-5 χ^2 | Bandpowers 1-9 χ^2 | Bandpowers 1-5 χ | Bandpowers 1-9 χ |
|------------------------------------------|----------------------------|----------------------------|--------------------------|--------------------------|
| Deck jackknife | | | | |
| EE | 0.046 | 0.030 | 0.164 | 0.299 |
| BB | 0.774 | 0.329 | 0.240 | 0.082 |
| EB | 0.337 | 0.643 | 0.204 | 0.267 |
| Scan Dir jackknife | | | | |
| EE | 0.483 | 0.762 | 0.978 | 0.938 |
| BB | 0.531 | 0.573 | 0.896 | 0.551 |
| EB | 0.898 | 0.806 | 0.725 | 0.890 |
| Tag Split jackknife | | | | |
| EE | 0.541 | 0.377 | 0.916 | 0.938 |
| BB | 0.902 | 0.992 | 0.449 | 0.585 |
| EB | 0.477 | 0.689 | 0.856 | 0.615 |
| Tile jackknife | | | | |
| EE | 0.004 | 0.010 | 0.000 | 0.002 |
| BB | 0.794 | 0.752 | 0.565 | 0.331 |
| EB | 0.172 | 0.419 | 0.962 | 0.790 |
| Phase jackknife | | | | |
| EE | 0.673 | 0.409 | 0.126 | 0.339 |
| BB | 0.591 | 0.739 | 0.842 | 0.944 |
| EB | 0.529 | 0.577 | 0.840 | 0.659 |
| Mux Col jackknife | | | | |
| EE | 0.812 | 0.587 | 0.196 | 0.204 |
| BB | 0.826 | 0.972 | 0.293 | 0.283 |
| EB | 0.866 | 0.968 | 0.876 | 0.697 |
| Alt Deck jackknife | | | | |
| EE | 0.004 | 0.004 | 0.070 | 0.236 |
| BB | 0.397 | 0.176 | 0.381 | 0.086 |
| EB | 0.150 | 0.060 | 0.170 | 0.291 |
| Mux Row jackknife | | | | |
| EE | 0.052 | 0.178 | 0.653 | 0.739 |
| BB | 0.345 | 0.361 | 0.032 | 0.008 |
| EB | 0.529 | 0.226 | 0.024 | 0.048 |
| Tile/Deck jackknife | | | | |
| EE | 0.048 | 0.088 | 0.144 | 0.132 |
| BB | 0.908 | 0.840 | 0.629 | 0.269 |
| EB | 0.050 | 0.154 | 0.591 | 0.591 |
| Focal Plane inner/outer jackknife | | | | |
| EE | 0.230 | 0.597 | 0.022 | 0.090 |
| BB | 0.216 | 0.531 | 0.046 | 0.092 |
| EB | 0.036 | 0.042 | 0.850 | 0.838 |
| Tile top/bottom jackknife | | | | |
| EE | 0.289 | 0.347 | 0.459 | 0.599 |
| BB | 0.293 | 0.236 | 0.154 | 0.028 |
| EB | 0.545 | 0.683 | 0.902 | 0.932 |
| Tile inner/outer jackknife | | | | |
| EE | 0.727 | 0.533 | 0.128 | 0.485 |
| BB | 0.255 | 0.086 | 0.421 | 0.036 |
| EB | 0.465 | 0.737 | 0.208 | 0.168 |
| Moon jackknife | | | | |
| EE | 0.499 | 0.689 | 0.481 | 0.679 |
| BB | 0.144 | 0.287 | 0.898 | 0.858 |
| EB | 0.289 | 0.359 | 0.531 | 0.307 |
| A/B offset best/worst | | | | |
| EE | 0.317 | 0.311 | 0.868 | 0.709 |
| BB | 0.114 | 0.064 | 0.307 | 0.094 |
| EB | 0.589 | 0.872 | 0.599 | 0.790 |

Splits the 4 boresight rotations

Amplifies differential pointing in comparison to fully added data. Important check of deprojection.



Splits by time

Checks for contamination on long (“Temporal Split”) and short (“Scan Dir”) timescales. Short timescales probe detector transfer functions.

Splits by channel selection

Checks for contamination in channel subgroups, divided by focal plane location, tile location, and readout electronics grouping

Splits by possible external contamination

Checks for contamination from ground-fixed signals, such as polarized sky or magnetic fields, or the moon

Splits to check intrinsic detector properties

Checks for contamination from detectors with best/worst differential pointing. “Tile/dk” divides the data by the orientation of the detector on the sky.

Calibration Measurements

For instance...

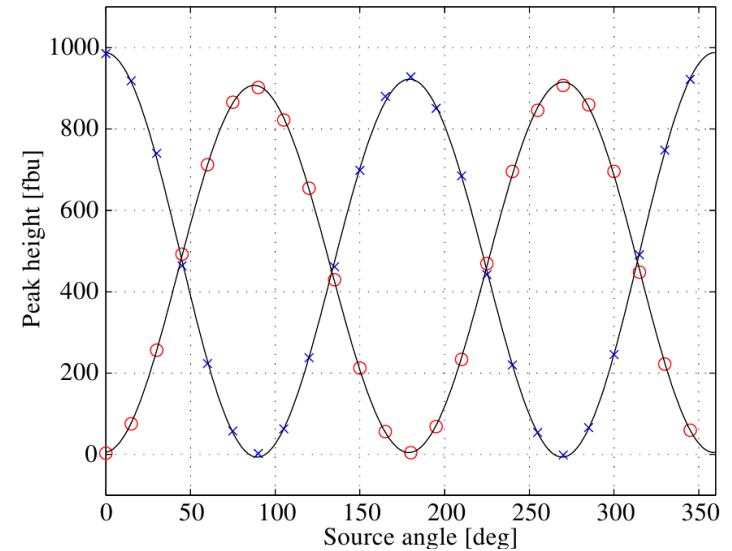
Far field beam mapping



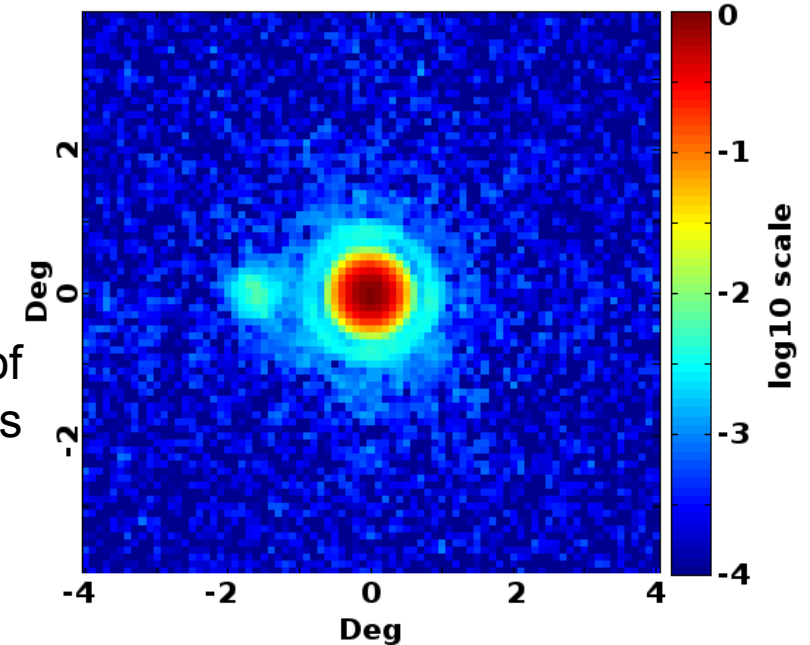
Detailed description in
Instrument Paper

Beam maps of
individual detectors

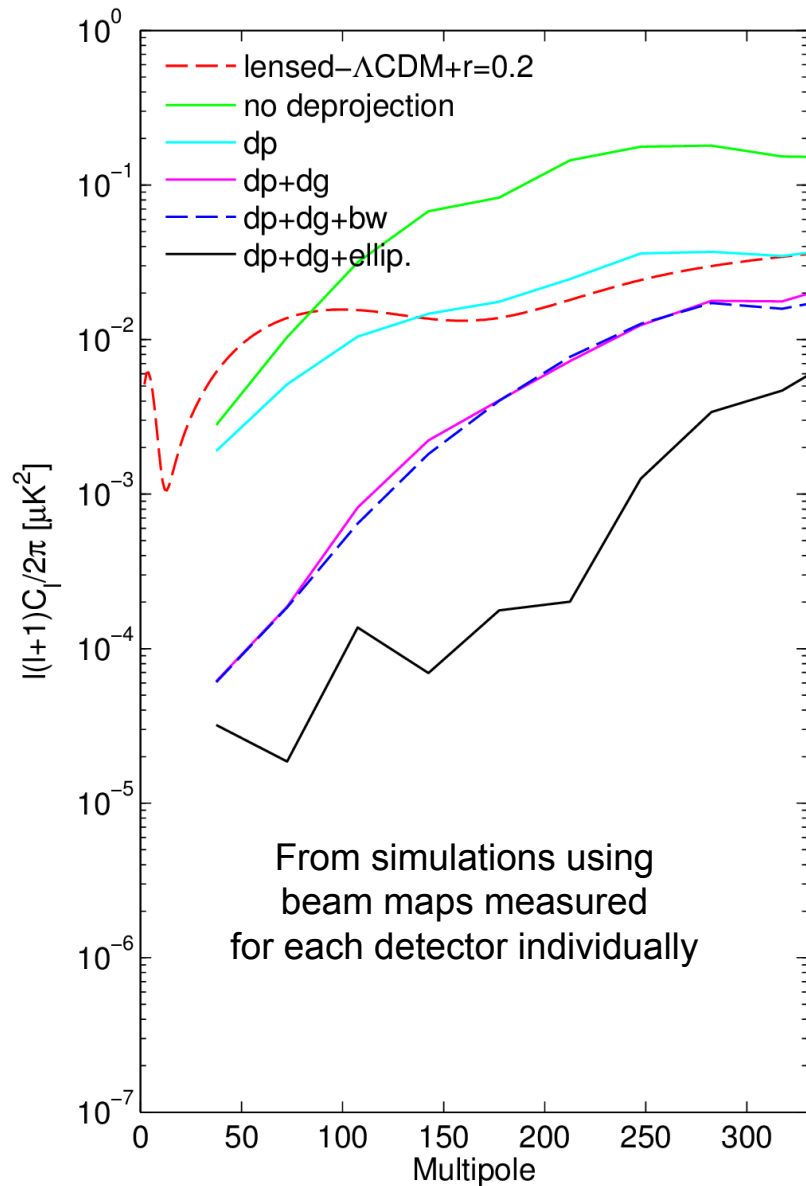
Detector Polarization Calibration



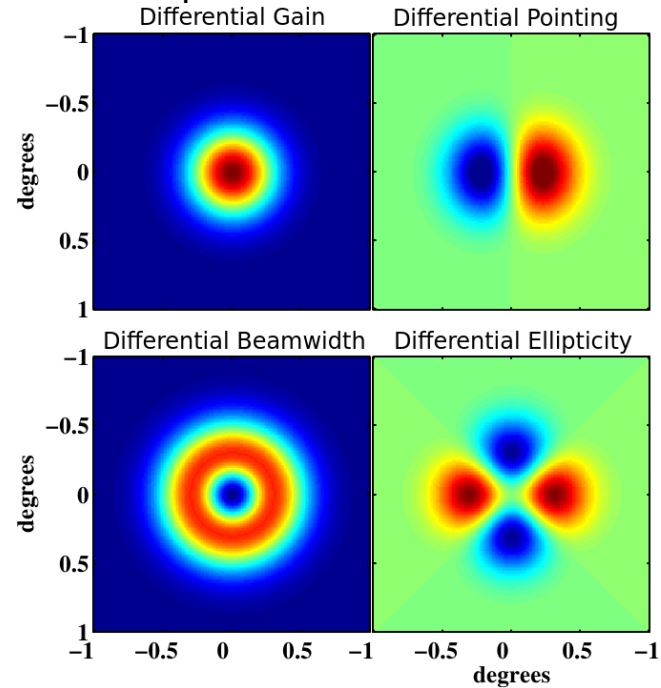
Channel 235



Systematics Removal: Deprojection



Technique developed to remove all types of leakage (false polarization) induced by differences of detector pair beam shapes

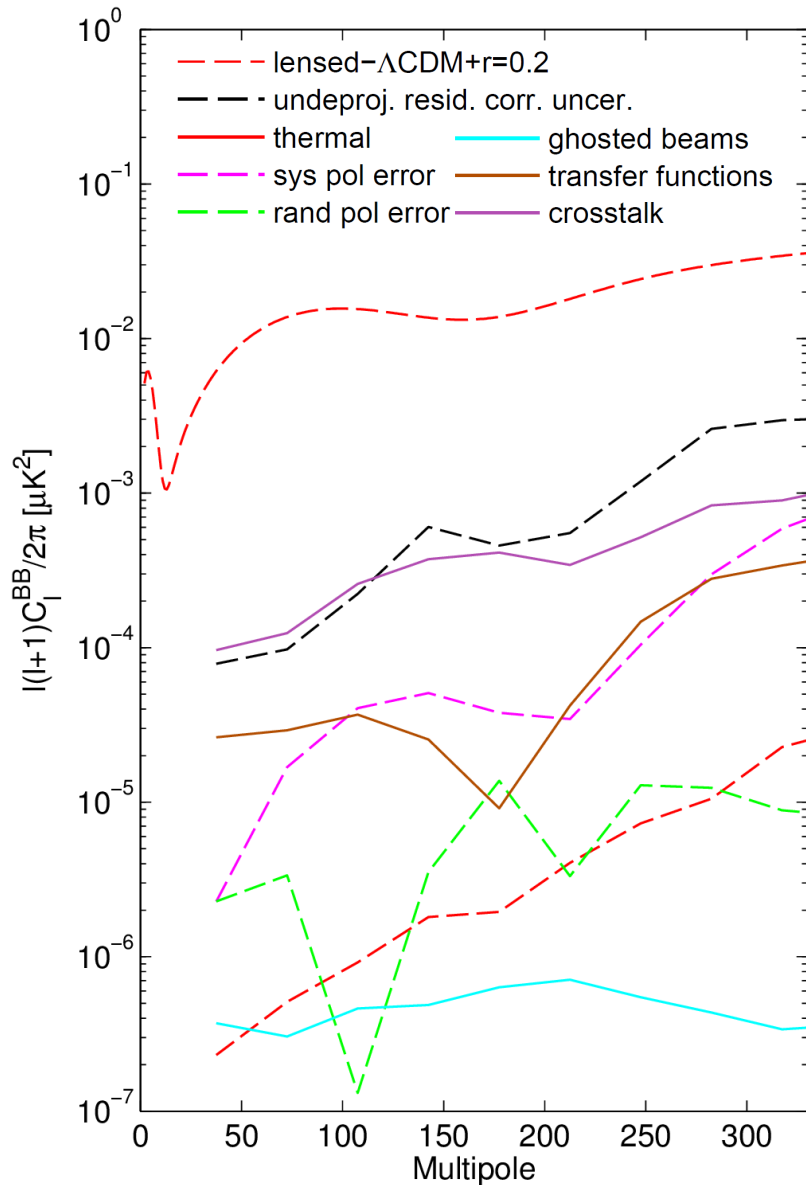


Use the Planck 143 GHz map to form template of the leakage

Deproject diff gain and pointing (& subtract measured diff ellipticity)

Subtract the residual (equiv to $r=0.001$) from the data

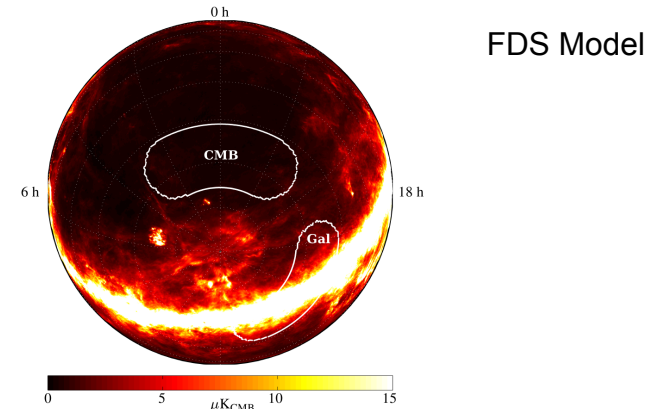
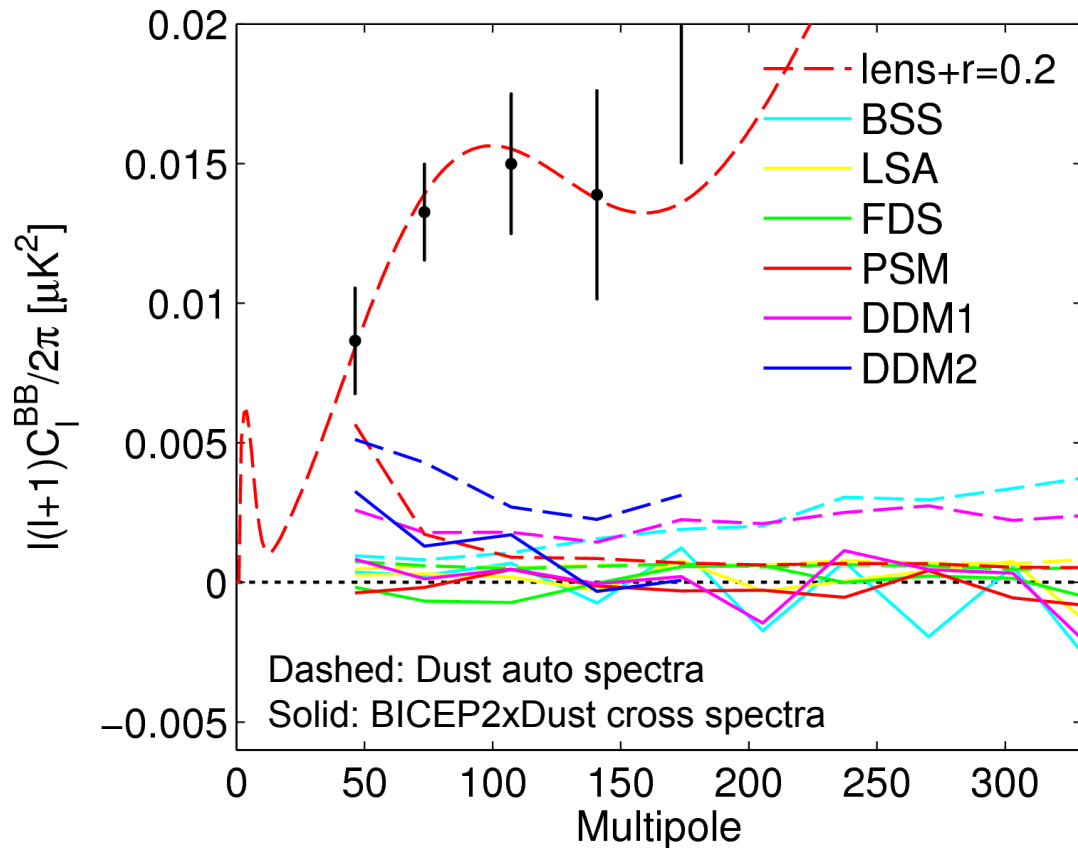
Systematics beyond Beam imperfections



All systematic effects that we could imagine were simulated based upon measured imperfections!

We find with high confidence that the apparent signal *cannot be explained* by instrumental systematics!

Polarized Dust Foreground Projections



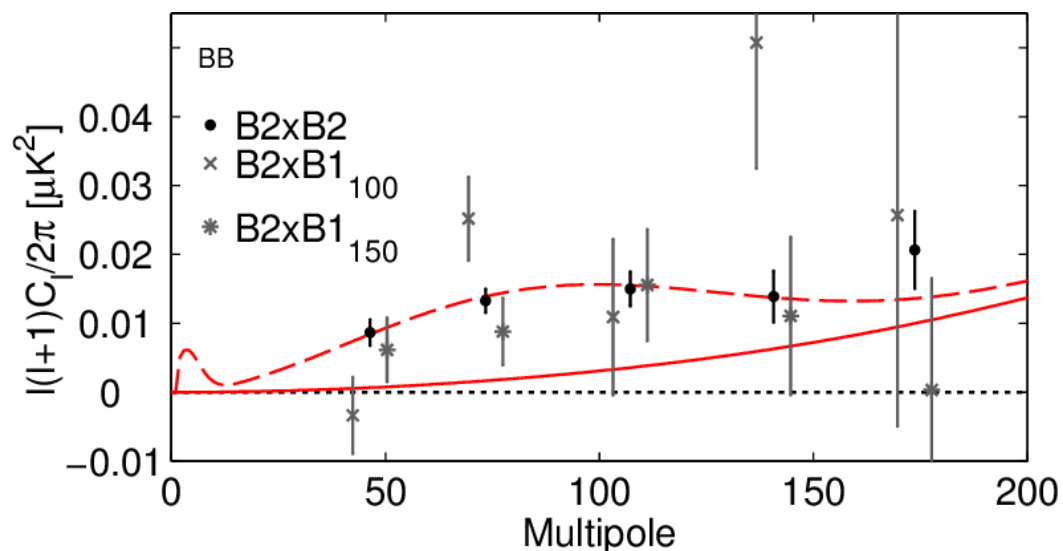
The BICEP2 region is chosen to have extremely low foreground emission.

Use various models of polarized dust emission to estimate foregrounds.

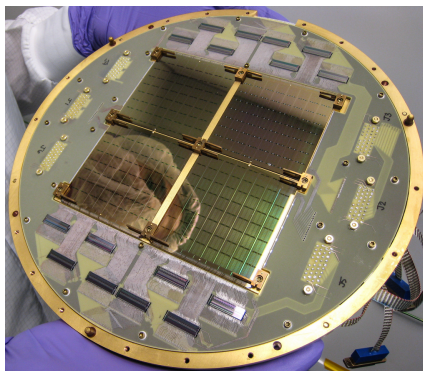
All dust auto spectra well below observed signal level.

Cross spectra consistent with zero.

Cross Correlation with BICEP1



Though less sensitive, BICEP1 applied **different technology** (systematics control) and **multiple colors** (foreground control) to the **same sky**.



BICEP2: Phased antenna array and TES readout
150 GHz

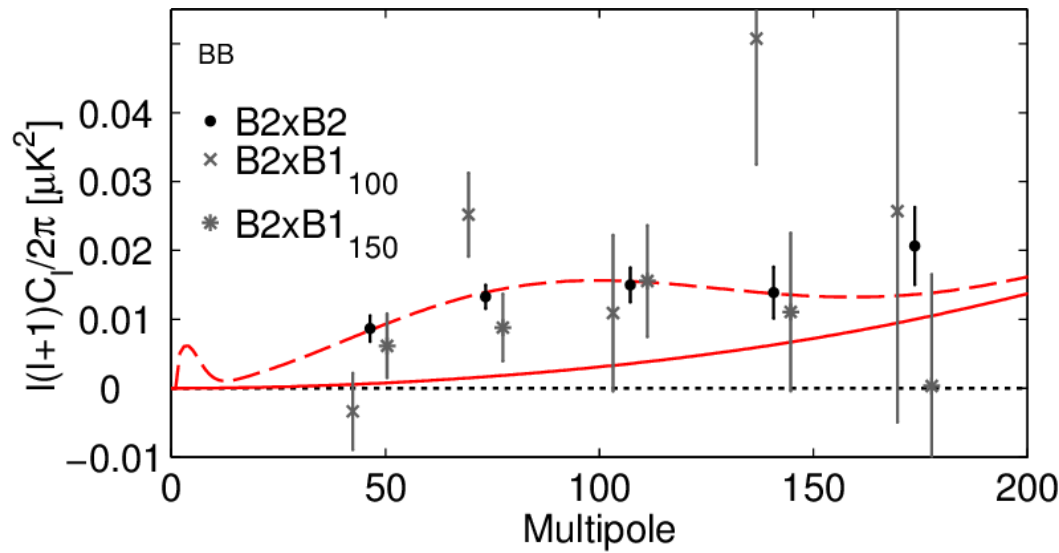
BICEP1: Feedhorns and NTD readout
150 and 100 GHz



Cross-correlations with both colors are **consistent** with the B2 auto spectrum

Cross with BICEP1₁₀₀ shows **$\sim 3\sigma$** detection of BB power

Spectral Index of the B-mode Signal



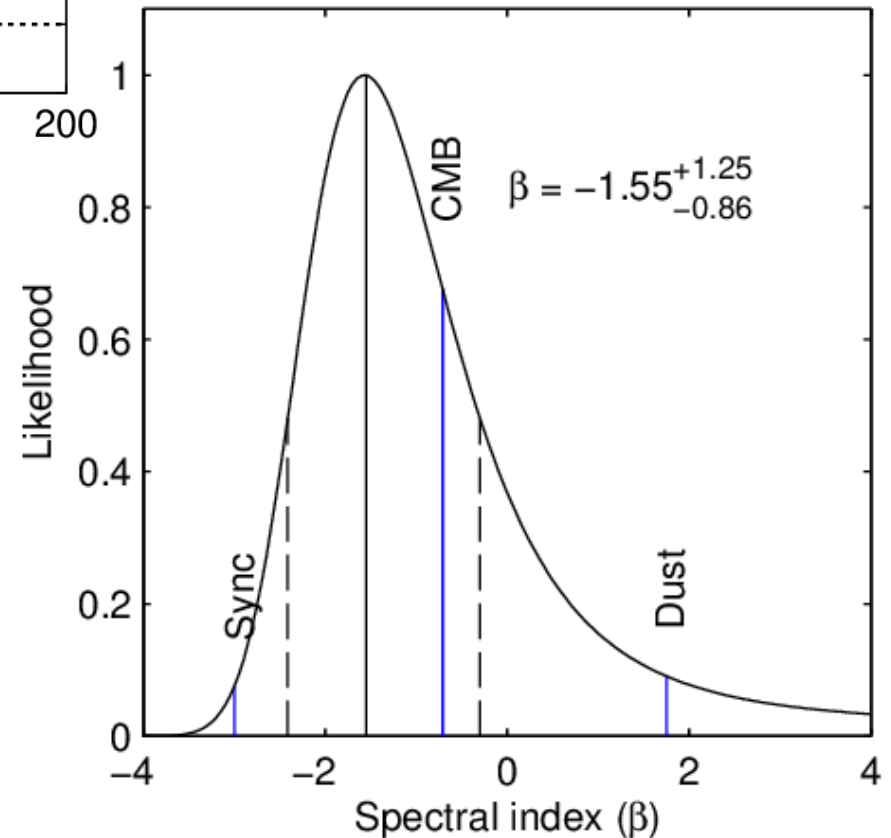
Likelihood ratio test: consistent with CMB spectrum, disfavor pure dust/sync at **2.2/2.3 σ**

Comparison of B2 auto with B2₁₅₀ × B1₁₀₀ constrains signal frequency dependence, independent of foreground projections

If **dust**, expect little cross-correlation

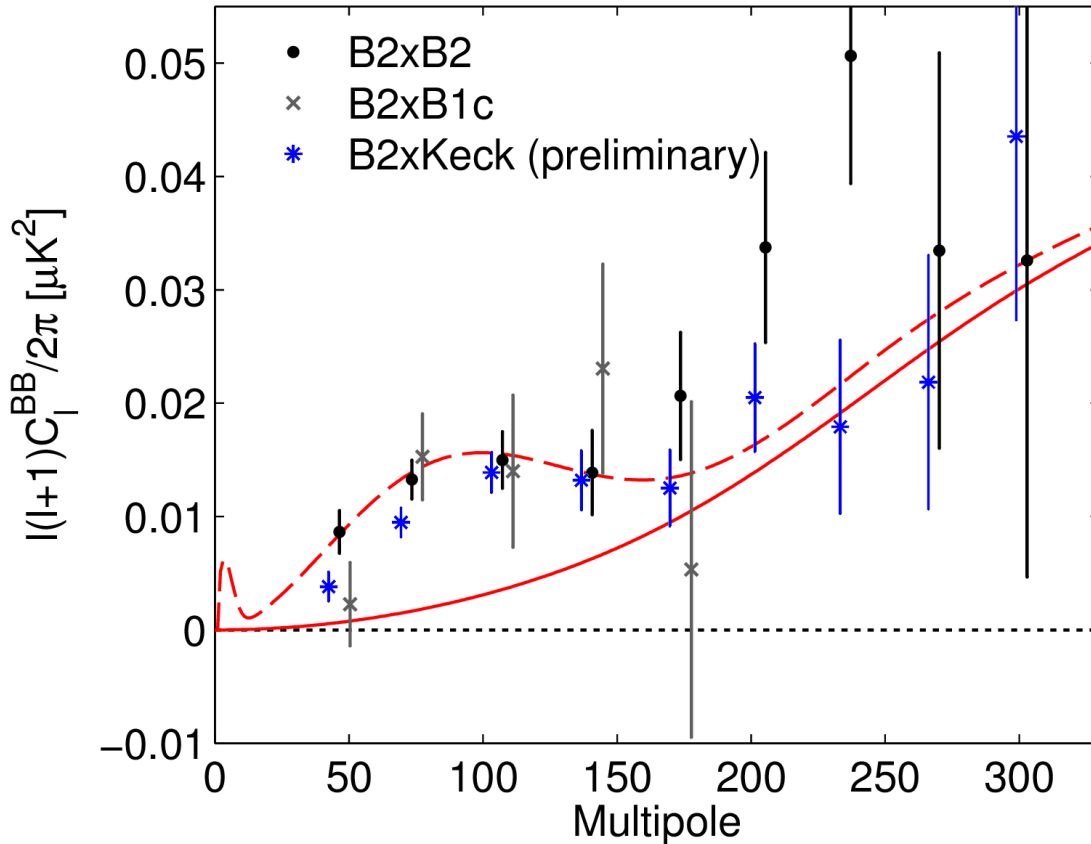
If **synchrotron**, expect bright correlation

Find **consistent with CMB**



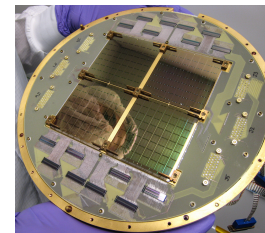
Cross Spectra between 3 Experiments

Form cross spectrum between BICEP2 and BICEP1 combined (100 + 150 GHz):



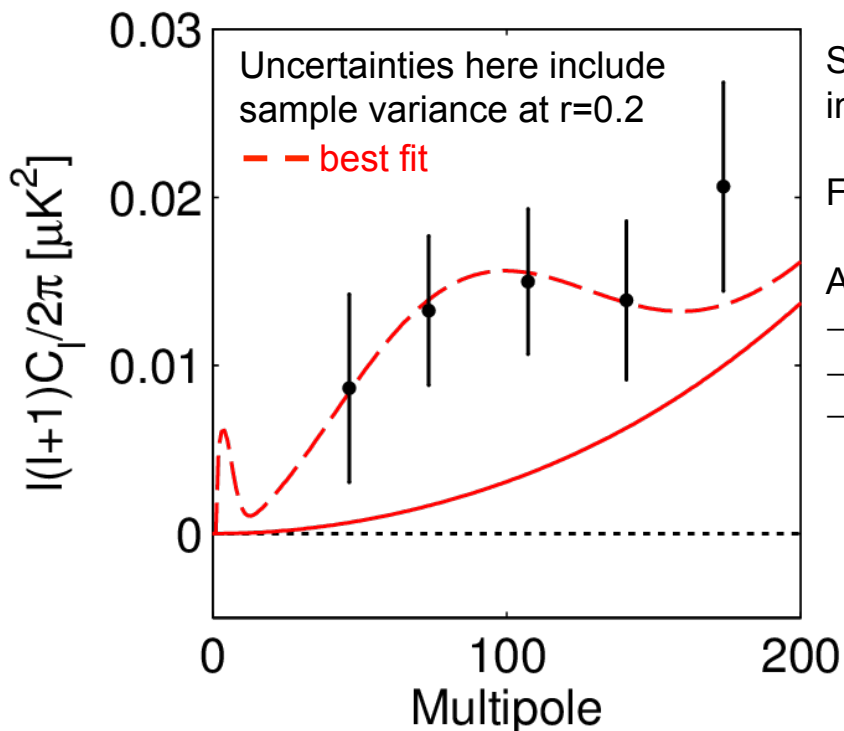
BICEP2 auto spectrum compatible with B2xB1c cross spectrum
~3 σ evidence of excess power in the cross spectrum

Additionally form cross spectrum with 2 years of data from *Keck Array*, the successor to BICEP2
Excess power is also evident in the B2xKeck cross spectrum



**Cross spectra:
Powerful additional evidence against a systematic origin of the apparent signal**

Constraint on Tensor-to-scalar Ratio r



Substantial excess power in the region where the inflationary gravitational wave signal is expected to peak

Find the most likely value of the tensor-to-scalar ratio r

Apply “direct likelihood” method, uses:

- lensed- Λ CDM + noise simulations
- weighted version of the 5 bandpowers
- B-mode sims scaled to various levels of r ($n_T=0$)

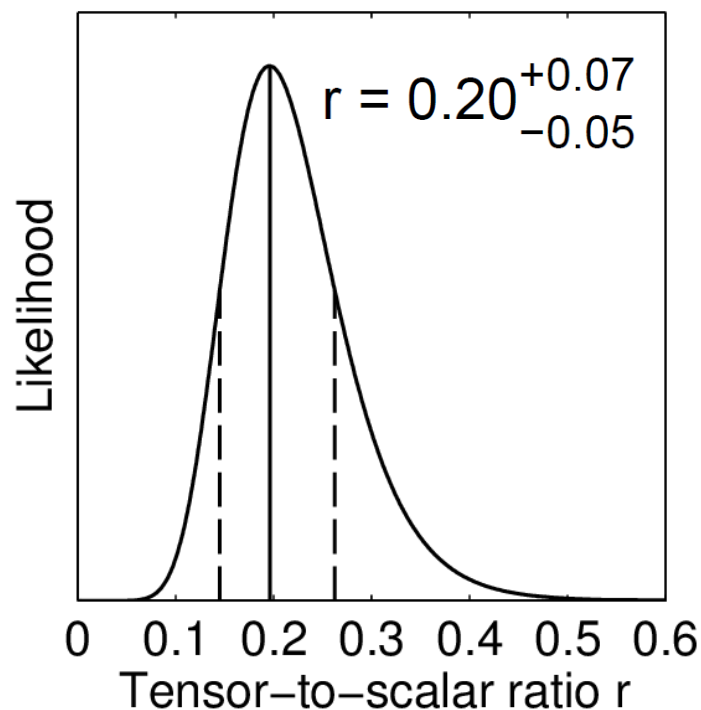
Within this simplistic model we find:

$r = 0.2$ with uncertainties dominated by sample variance

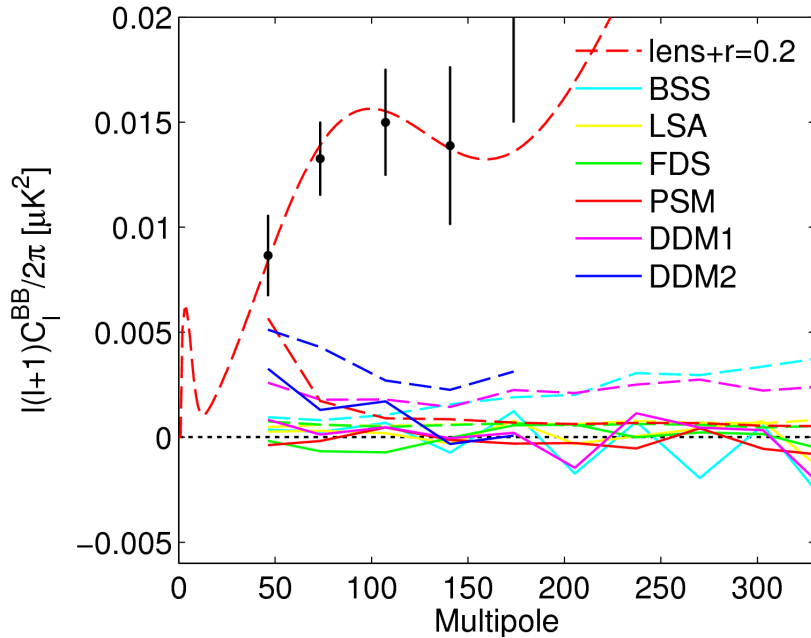
PTE of fit to data: 0.9

→ model is perfectly acceptable fit to the data

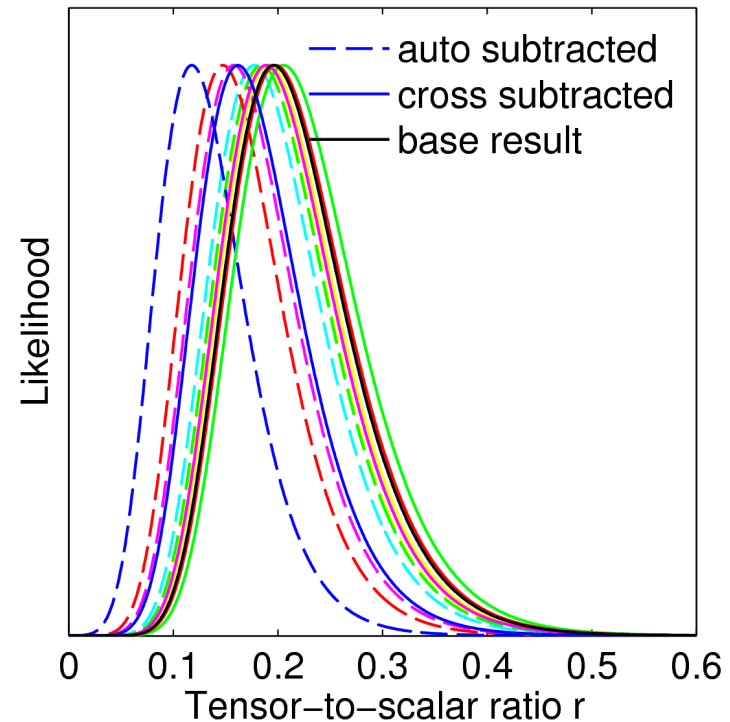
$r = 0$ disfavored at 7.0σ



Constraint on r under Foreground Projections



Adjust likelihood curve by subtracting the dust projection auto and cross spectra from our bandpowers:



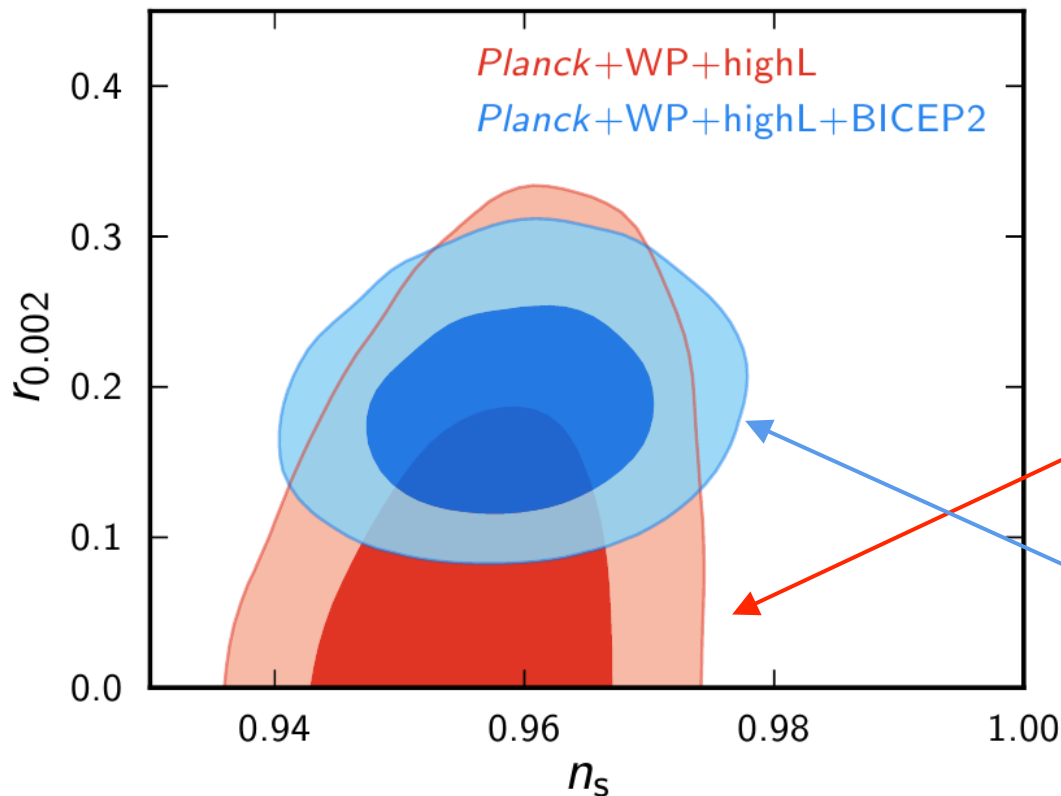
Probability that each of these models reflect reality hard to assess

DDM2 uses all publicly available information from Planck - modifies constraint to $r = 0.16^{+0.06}_{-0.05}$
 $r = 0$ still disfavored at 5.9σ

Dust contribution is largest in the first bandpower. Deweighting this bin would lead to less deviation from our base result.

Compatibility with Indirect Limits on r

Constraint on r with running allowed:



Indirect limit on r from combination of temperature data over a wide range of angular scales:

SPT+WMAP+BAO+ H_0 : $r < 0.11$

Planck+SPT+ACT+WMAP_{pol} : $r < 0.11$

This apparent tension can be relieved with various extensions to lensed Λ CDM.

Example: running of the spectral index

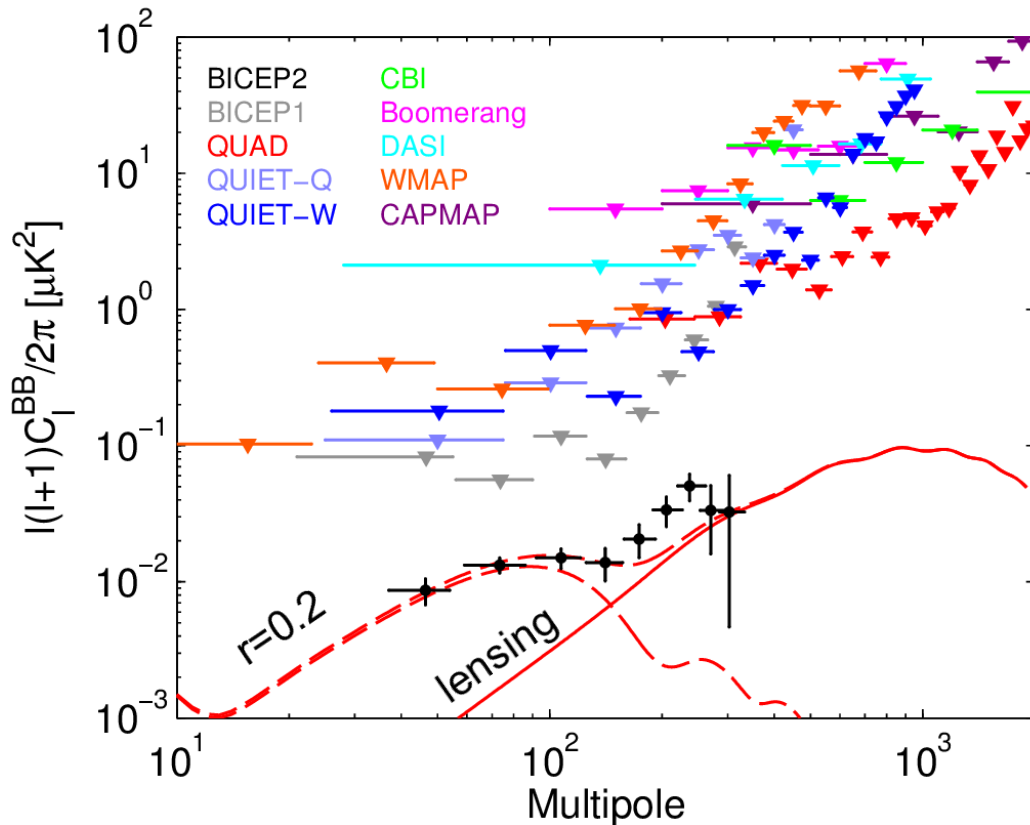
Planck likelihood chains for lensed Λ CDM + *tensors* + *running*

Same chains, importance sampled with the BICEP2 r likelihood

Other possibilities within Λ CDM?...

Conclusions

BICEP2 and upper limits from other experiments:



Consistent with expectations for **primordial gravitational waves** from **GUT-scale inflation**

Most sensitive polarization maps ever made

Power spectra perfectly consistent with lensed Λ CDM except:
5.2 σ excess in the B-mode spectrum at low multipoles ($l \sim 100$)!

7 σ preference for non-zero r above lensed Λ CDM

Extensive studies and jackknife test strongly argue against systematics as the origin

Foregrounds do not appear to be a large fraction of the signal:

- foreground projections
- lack of cross correlations
- CMB-like spectral index
- shape of the B-mode spectrum

Constraint on tensor-to-scalar ratio r in simple inflationary gravitational wave model:

$$r = 0.20^{+0.07}_{-0.05}$$